AD-A111 492 SAN ANTONIO AIR LOGISTICS CENTER KELLY AFB TX F/G 1/3
OV-10A NOSE GEAR FORK DAMAGE TOLERANCE ANALYSIS,(U)
JAN 82 K F BARNES, J L HAINES
UNCLASSIFIED SA-ALC/MM-7588 NL

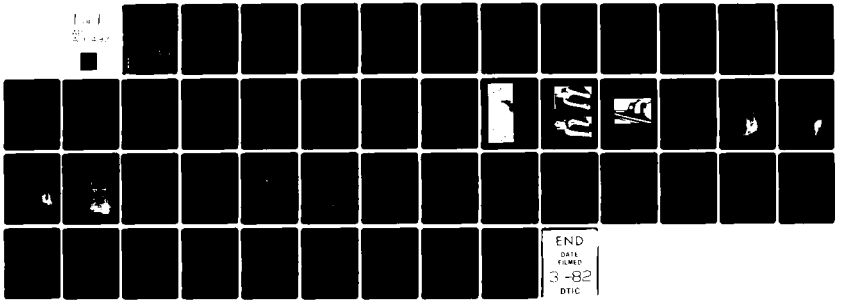

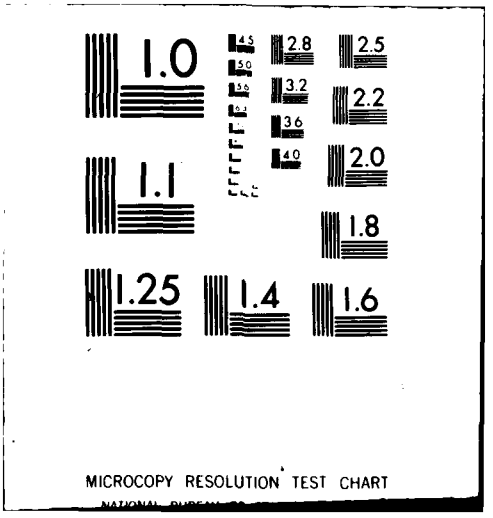
1.0
1.1
1.25
1.4
1.6
1.8
2.0
2.2
2.5
2.8
3.2
3.6
4.0
4.5
5.0
5.6
6.3
MICROCOPY RESOLUTION TEST CHART

SA-ALC/MM-7588

(11)

AD A111492

OV-10A NOSE GEAR FORK
DAMAGE TOLERANCE ANALYSIS

Kenneth F. Barnes, Capt, USAF
James L. Haines, Capt, USAF
Damage Tolerance Analysis Unit
San Antonio Air Logistics Center/MMSRE

January 1982

SECURITY CLASSIFICATION OF THIS PAGE (When Data Entered)

REPORT DOCUMENTATION PAGE	READ INSTRUCTIONS BEFORE COMPLETING FORM
1. REPORT NUMBER: SA-ALC/MM-7588	2. GOVT ACCESSION NO.: AD-A111 492
3. RECIPIENT'S CATALOG NUMBER:	
4. TITLE (and Subtitle): OV-10A NOSE GEAR FORK DAMAGE TOLERANCE ANALYSIS	5. TYPE OF REPORT & PERIOD COVERED: Final August 1980 - Sep 1981
	6. PERFORMING ORG. REPORT NUMBER:
7. AUTHOR(s): Kenneth F. Barnes, Capt, USAF James L. Haines, Capt, USAF	8. CONTRACT OR GRANT NUMBER(s):
9. PERFORMING ORGANIZATION NAME AND ADDRESS: SA-ALC/MMSRE Kelly AFB TX 78241	10. PROGRAM ELEMENT, PROJECT, TASK AREA & WORK UNIT NUMBERS:
11. CONTROLLING OFFICE NAME AND ADDRESS: SA-ALC/MMSRE Kelly AFB TX 78241	12. REPORT DATE: January 1982
	13. NUMBER OF PAGES:
14. MONITORING AGENCY NAME & ADDRESS(if different from Controlling Office):	15. SECURITY CLASS. (of this report): UNCLASSIFIED
	15a. DECLASSIFICATION/DOWNGRADING SCHEDULE:

16. DISTRIBUTION STATEMENT (of this Report)

Approved for public release, distribution unlimited.

17. DISTRIBUTION STATEMENT (of the abstract entered in Block 20, if different from Report)

18. SUPPLEMENTARY NOTES

19. KEY WORDS (Continue on reverse side if necessary and identify by block number)

OV-10A	Crack Growth	7075-T73
Nose Gear Fork	Stress Spectrum	Finite Element
Landing Gear	Landing Load History	Analysis
Damage Tolerance Analysis	Residual Strength	
Initial Flaws	Stress Gradient Correction Factor	

20. ABSTRACT (Continue on reverse side if necessary and identify by block number)

A limited Damage Tolerance Analysis (DTA) of the OV-10A nose gear fork was performed to determine the fracture characteristics at a location on the underside of the fork in a machined fillet radius just aft of the jack point. The analysis included determination of a landing load history, finite element stress analysis, stress spectrum development, stress intensity solution, crack growth analysis, and residual strength calculations.

DD FORM 1 JAN 73 1473 EDITION OF 1 NOV 65 IS OBSOLETE

SECURITY CLASSIFICATION OF THIS PAGE (When Data Entered)

OV-10A NOSE GEAR FORK

DAMAGE TOLERANCE ANALYSIS

January 1982

Prepared by:

Kenneth F. Barnes, Capt, USAF

James L. Haines, Capt, USAF

Reviewed by:

Joseph A. Ori, Major, USAF
Chief, Damage Tolerance Analysis

Juan J. Saenz,
Chief, Aeronautical Section

Approved by:

Kenneth W. Mays, Col, USAF
Chief, System Management Division
Directorate of Materiel Management

Table of Contents

List of Figures

List of Tables

List of Symbols

A	A point at the maximum depth of the crack front
a	Crack depth
B	A point where the crack front intersects the surface of the material
C	Forman Equation constant factor
c	Half the crack surface length
da/dn	Crack growth rate, inches per cycle
K_A	Stress intensity at point A (depth of crack)
K_B	Stress intensity at point B (surface of crack)
K_{IC}	Plane strain fracture toughness
L-S	Loading parallel to longitudinal grain direction, crack growing in short tranverse direction
L-T	Loading parallel to longitudinal grain direction, crack growing in long tranverse direction
n	Forman Equation exponent
P	Drag brace axial load
Q_Z	Oleo axial load
Rx,Rz	X and Z components of load at fork axle, X and Z are aircraft coordinates
R1,R2	Components of load at fork axle relative to fork
S-T	Loading parallel to short tranverse grain direction, crack growing in long tranverse direction
T-L	Loading parallel to long tranverse grain direction, crack growing in longitudinal direction
t	Thickness of material
w	Width of material
ΔK	Delta stress intensity; difference between stress intensity calculated at maximum and minimum stresses of a stress cycle
σ	Stress

σ_{p_a}	Principal stress at a distance a into the thickness of a plate remote from a surface crack of depth a, and perpendicular to the crack face
σ_{p_c}	Principal stress at the surface of a plate a distance c from the centerline of the plate and remote from a center surface crack of length 2c, and perpendicular to the crack face
$\sigma_{p_{9141}}$	Principal stress at GRID 9141 perpendicular to the crack face
σ_x, σ_y, σ_z	Components of normal stress
$\tau_{xy}, \tau_{yz}, \tau_{zx}$	Components of shear stress

1.0 SUMMARY

A limited Damage Tolerance Analysis (DTA) of the OV-10A nose gear fork was performed to determine fracture characteristics at a location on the underside of the fork in a machined fillet radius just aft of the jack point. The analysis included determination of a landing load history, finite element stress analysis, stress spectrum development, stress intensity solution, crack growth analysis, and residual strength calculations. The finite element analysis was performed by Captain Jim Haines. Captain Ken Barnes developed the spectrum and performed the fracture analysis. This work was begun in August 1980 and completed in September 1981.

2.0 INTRODUCTION

This report presents the DTA of the OV-10A nose gear fork. An OV-10A sustained a failure of the fork while making a short field landing. The metallurgical report (Reference 1) indicated the failure was primarily due to a fatigue crack located in the fillet radius just aft of the jack point on the underside of the fork. This crack is located at arrow A in figure 1. Figure 2 shows a magnified view of this same crack. Arrow B points to a long shallow crack which is enlarged in figure 3. This crack, which originated from a tool mark, was not considered to be the primary cause of failure in the metallurgical report. The two cracks were not on the same plane, but the final fracture broke both of these cracks open.

The nose gear fork is a 7075-T73 aluminum forging. Photographs of the fork are in figures 4 and 5, and figure 6 is a close-up view of the analysis location. Figure 7 shows the entire nose gear assembly.

The fork was modeled using NASTRAN finite elements to determine the principal stresses and stress gradients in the analysis location. The results of the NASTRAN analysis were used in stress spectrum generation and the stress intensity solution.

The stress spectrum is based on both the drop test portion of the OV-10A full scale fatigue test and on instrumented landing tests for various runway types and landing attitudes.

The crack growth analysis used a modified version of a crack growth program developed by the McDonnell Aircraft Company (MCAIR) under contract to the Air Force Flight Dynamics Laboratory (Reference 2). The program was modified to incorporate spectrum loading, the stress gradient correction factors, and calculation of incremental crack growth by a Forman equation rather than by a table of log da/dN versus logΔK.

Fracture data for 7075-T73 forged material was obtained from references 3 and 4.

The crack growth analysis shows very long crack growth lives when subjected to spectrum loading representative of the full scale fatigue testing. The fork was analyzed for five types of initial flaws with the tool mark type being the most severe case.

3.0 ANALYSIS PROCEDURES

3.1 STRESS ANALYSIS

The objective of the stress analysis was to determine the principal stresses and stress gradients in the OV-10A nose landing gear fork in the radius just aft of the nose gear jack point for use in crack growth studies. A finite element model of the fork was developed for use with NASTRAN and sample loads were applied to the model at the axle to determine unit stresses in the critical radius. A computer program called SPECFORK was developed to convert the landing gear loading spectrum into equivalent loads at the fork axle, and, using the NASTRAN unit stresses, calculate the principal stresses in the area of the radius. These stress calculations were used to generate a stress spectrum at the radius and accompanying through the thickness and surface stress gradients for use in crack growth studies.

The nose landing gear fork is basically symmetrical about its longitudinal (X) axis, and hence only the half containing the nose gear jack point was modeled. The geometry for the model was obtained from two sources. The primary source was the engineering drawings for the fork. When engineering drawings were insufficient, direct measurements were taken from an actual fork. Direct measurements were also used where substantial differences occurred between these two sources. The actual fork had a 2.0 inch lightening hole, while the drawing shows a 1.5 inch lightening hole. The fork which failed had a 2.0 inch hole, so the 2.0 inch lightening hole configuration was modeled. (The lightening hole is visible in figures 4 and 5.) Figures 8 through 11 display the final NASTRAN model and the orientation of the coordinate system. The coordinate system used for the model is the same as used in the engineering drawings.

The GIFTS finite element program was used as an aid to plot and generate grid points. The grid points were then converted to a format acceptable to NASTRAN. The remainder of the model was built for execution with NASTRAN by using a program called NASCAR (NASTRAN Cards) to format the NASTRAN input and by plotting the model for checkout using the EZPLOT and MENU programs. The linear isoparametric hexahedron element, CIHEX1, is used wherever possible. CHEXA1 elements are used only in the prong of the fork. CWEDGE and CTETRA elements are used where necessary to describe and blend the overall shape. CTRIA2 elements were used only to model the forward lug which attaches to the nose gear oleo cylinder for load transfer purposes.

To simulate symmetry, all GRIDs along the longitudinal plane of symmetry (Y=0) were constrained for Y translations and for rotations about the X and Z axes. Constraints in both the X and Z directions were added to selected GRIDs on the inside of the upper lug which attaches to the nose gear oleo piston to simulate the effects of a stationary pin. To prevent the model from rotating about this pin, the forward lug which attaches to the nose gear oleo cylinder was also constrained in the Z direction.

Loads were applied at the tip of the fork prong which represents the wheel axle. The loading cases run in NASTRAN included loads applied parallel to the fork prong (X direction), perpendicular to the fork prong (Z direction), and as a linear combination of the two.

Figure 12 shows a cross section of the critical areas as modeled in NASTRAN. The circled numbers indicate element ID numbers. All others are GRID ID numbers. The crack to be studied is assumed to be growing in the YZ plane with its center at GRID 9141. Stress output from NASTRAN for this area consists of normal stresses (σ_x, σ_y, σ_z) and shear stresses (τ_{xy},τ_{yz},τ_{zx}) at all of the GRID points and at all of the element centroids.

NASTRAN loading case #4 (-15,000 lb in X direction) was used to determine unit normal and shear stresses due to a one pound load in the X direction by dividing the stresses by -15000. Table 1 lists these stresses for the critical area. Loading case #2 (15,000 lb in Z direction) was similarly used to determine the unit normal and shear stresses due to a one pound load in the Z direction. Table 2 lists these stresses for the critical area. Spot checks of the other loading cases confirmed that these unit stress components remained constant with varying load values and combinations.

Figure 13 is a schematic of the OV-10 nose landing gear assembly and the axis system used to describe its geometry. Since the fork orientation varies with the oleo strut compression, the axes used to describe the fork NASTRAN model will not generally coincide with the axes used to describe the landing gear assembly.

The landing loads measured in the instrumented landing tests were defined in terms of the loads P and Q_z and a compression distance for the oleo strut. This information along with the fork geometry are used in the computer program, SPECFORK, to solve for reactions R_x and R_z at the fork axle. These reactions are in turn resolved into the fork model axis system as a load, R1, at the axle and parallel to the fork prong (X axis) and as a load R2, perpendicular to the fork prong (Z axis). The derivations of these equations are found in MMSRE project folder 81-355A.

Shear and normal stresses for any combination of R1 and R2 were determined by the process of superposition in SPECFORK by summing R1 times the unit stresses due to a load in the X direction with R2 times the unit stresses due to a load in the Z direction. When expressed in tensor form, these stresses were then used to calculate the three principal stresses and unit vectors by solving for the eigenvalues and eigenvectors of the tensor.

The principal stresses obtained by using the NASTRAN stress output from GRID 9141 proved to be higher than the principal stresses derived by extrapolating from element centroids. Hence, to remain conservative, the SPECFORK output using the unit normal and shear stresses from GRID 9141 was used to calculate the principal stress spectrum for the center of the crack. Only the principal stress which is primarily perpendicular to the crack plane is used.

The stress gradients, on the other hand, were derived by averaging the stress output at the centroids of the elements. Figure 14 is a plot of the principal stresses versus crack depth for various representative ratios of R1 and R2 and normalized to the principal stress at GRID 9141. For simplicity, a linear gradient was assumed so that:

$$\sigma_{p_a} = \sigma_{p_{9141}} \times (1.0 - 1.7878a) \quad \text{for } a \leq .2$$

$$\sigma_{p_a} = .6424 \times \sigma_{p_{9141}} \quad \text{for } a > .2$$

where a = crack depth.

Figure 15 is a plot of the principal stresses versus half crack surface length for the same ratio of R1 and R2 and normalized to the principal stress at GRID 9141. A linear gradient is again assumed, and it is also assumed symmetrical about the crack center so that:

$$\sigma_{p_c} = \sigma_{p_{9141}} \times (1.0 + .2514c)$$

where c = half crack surface length.

3.2 STRESS SPECTRUM

A stress spectrum was developed for use in calculating crack growth in the critical location of the OV-10A nose gear fork. The spectrum is based on the OV-10A landing load spectrum used in the drop test portion of the full scale fatigue test (Reference 5). Nose gear loads for various landing attitudes and runway types were obtained from instrumented landing tests reported in Reference 6.

The drop test spectrum was defined in terms of numbers of landings for different sink speeds and landing attitudes for four different runway types. The first runway type is level, while the other three were rough types A, B, and C. Type A had a three inch raised step, type B had a four inch bump, and type C had a four inch deep trough. Roughness types B and C were grouped together in the drop tests. The landing attitude types were "two wheels tail down," "three wheels level," "pitch and roll," and "nose down." The gross weight of the test airplane for the second 7500 hours of testing was 10,044 lbs, and the sinking speeds ranged from 11.5 to 20.8 ft/sec. This 7500 hour drop test spectrum consisted of 4608 landings, of which 2585 were for the level terrain category, 489 for roughness type A, and 1534 for a combination of roughness types B and C. The same mix was used in the stress spectrum: 56.1% level, 10.6% type A, and 33.3% type B and C combined.

The landing tests had six landings for the level terrain category, 23 for roughness types B and C and 13 for roughness type A. The sink speeds ranged from 9.8 to 17.9 ft/sec. The loads data for these landing tests consisted of oscillograph time traces of oleo axial load, drag brace axial load, and the oleo stroke (see figure 16 for an example). Values of these three parameters were read from the traces for time slices which occurred at minimum and maximum values of the load parameters where it seemed likely that stress peaks and valleys would occur. After stresses were determined for each time slice based on the finite element model, the locations and values of peak and valley stresses were determined. These values were tabulated and used to determine frequency of occurrence of different stress levels by terrain category. Based on the mix of landing types in the preceding paragraph, the tables of occurrences were representative of 561 landings on level terrain, 106 on type A rough terrain, and 333 on types B and C rough terrain (see tables 3 through 5). The total spectrum was thus representative of 1000 landings. The maximum spectrum stress is 28 ksi.

These tables served as input to program ACEY which was used to generate a random landing by landing stress spectrum representative of 1000 landings. The resulting stress history was then range pair cycle counted by program RPCM. The resulting analysis spectrum was then reformatted for input to a crack growth program. The 1000 landing spectrum is called a block and is repeated as many times as necessary during the crack growth calculations. (One block of 1000 landings is approximately equivalent to 1628 flight hours based on the ratio of flight hours to landings in the drop test spectrum.)

3.3 STRESS INTENSITY SOLUTION

The analysis assumed a semielliptical surface flaw of depth a and length 2c as shown in figure 17. A slice synthesis method of determining stress intensity at both the depth (point A) and surface (point B) of the flaw was used. This method was developed by MCAIR and is reported in Reference 2. This method calculates two correction factors, BETAA and BETAB. Both are functions of a, c and the the thickness of the material, t. In addition to these two correction factors, two more correction factors were used to account for stress gradients determined from the finite element analysis. Referring back to section 3.1,

$$BETATG = \frac{\sigma_{p_a}}{\sigma_{p_{9141}}}$$

$$= 1.0 - 1.7878\,a \quad \text{for } a \leq .2$$

$$= .6424 \quad \text{for } a > .2$$

and

$$BETASG = \frac{\sigma_{p_c}}{\sigma_{p_{c9141}}}$$

$$= 1.0 + .2514c$$

BETATG corrects stress intensity for the stress gradient through the thickness, and BETASG corrects for the stress gradient along the surface away from the center of the crack (c = 0). The stress intensity solution for the crack front at point A is:

$$K_A = \text{BETAA} \times \text{BETATG} \times \sigma \sqrt{\pi a}$$

and the stress intensity solution for the crack front at point B is:

$$K_B = \text{BETAB} \times \text{BETASG} \times \sigma \sqrt{\frac{\pi c}{\cos\left(\frac{\pi c}{w}\right)}}$$

where w is the width of the material in the crack surface direction.

These stress intensity solutions were used in both the crack growth program and a residual strength calculation program.

3.4 FRACTURE DATA

The OV-10 nose gear fork is a 7075-T73 forging. Fracture data for this material was obtained from References 3 and 4. Since surface flaws were analyzed, plain strain was assumed. Plane strain fracture toughness (K_{IC}) values for various load to crack orientations are as follows:

45 KSI $\sqrt{in}$ L-T

28 KSI $\sqrt{in}$ S-T

19 KSI $\sqrt{in}$ T-L

Metallurgical analysis of the analysis location shows the grain orientation to be parallel to the principal load and perpendicular to the crack face. This means that L-T and/or L-S fracture data are appropriate. The crack growth rate data used was for the L-T direction, but critical crack size and residual strength calculations assumed a K_{IC} for the T-L direction. This was because the service failure indicated the fracture toughness may have been low. Using a low value of K_{IC} in the analysis was an attempt to explain the service failure due to the small crack size present in the failed fork.

Crack growth rate data was obtained from References 2 and 3 for stress ratios of 0.88 and 0.33. Both data sets were for L-T grain orientation, low humidity air, and room temperature conditions. A Forman equation was derived to predict da/dn vs K for these two stress ratios. The Forman equation is as follows:

$$da/dn = \frac{C \Delta K^n}{(1-R) K_{IC} - \Delta K}$$

where $C = 7.234 \times 10^{-7}$

$n = 2.5$

$K_{IC} = 45.0$

3.5 INITIAL FLAW ASSUMPTIONS

Crack growth calculations were made for five different initial flaw sizes. The types and their dimensions in inches are as follows:

	a	c
service failure	.01	.0705
corrosion pit	.01	.01
mechanical damage	.02	.125
forging lap	.02	.05
tool mark	.019	.25

The definitions of a and c are illustrated in Figure 17.

The dimensions for the corrosion pit, mechanical damage, and forging lap initial flaws are from the Reference 2 report and are based on a field survey conducted by AFFDL and McDonnell Douglas at Ogden ALC. This survey also defined a tool mark type initial flaw of depth .003 inch, but a study of residual strength curves for a range of crack depths from .003 inch to .1 inch and surface lengths of .5 inch and .3 inch revealed that the stress intensity solution was invalid for a/c ratios less than about .07. This is due to BETAA values becoming very large in this region. Therefore, a depth of .019 was assumed for the tool mark flaw.

The service failure initial flaw is based on the dimensions of the fatigue crack believed to have caused the service failure. The failure size was measured to be .024 inch deep and .15 inch long (a = .024, c = .075). Using the surface flaw growth analysis routine in Reference 2, the failure size flaw was grown under constant amplitude loading to obtain a plot of a versus c. This plot was then extrapolated back to a smaller crack size (a = .01, c = .0705) and then grown with the same routine to confirm that it would pass through the failure size point. This smaller size was then used as an assumption for the initial crack dimensions for the service failure initial flaw.

3.6 CRACK GROWTH ANALYSIS

The crack growth analysis was performed using a modified version of the surface flaw growth analysis routine in Reference 2. This program calculates growth of surface flaws both through the thickness and along the surface. This program does not take into account retardation caused by overloads. The slice synthesis method is used to calculate BETAA and BETAB, the correction factors at the depth and surface respectively. The program was modified to include the depth and surface stress gradient correction factors, BETATG and BETASG. Other modifications include capability to accept spectrum loads and to integrate crack growth by means of a Forman equation.

The analysis shows crack growth lives in excess of 30,000 landings for all five initial flaw types when subjected to the analysis spectrum. Only the tool mark crack, which had the highest crack growth rate, was continued beyond 30,000 landings. It reached failure at about 37,300 landings. The other flaw types have lives in excess of this.

The service failure flaw reached the size where failure had occurred in the field at 17,600 landings, but the analysis does not show a failure at this point or before 30,000 landings. The first 30 blocks (30,000 landings) are plotted for four of the five flaw types, and the crack growth curve for the tool mark is plotted from initial size to failure at 37,300 landings (see figures 18 and 19).

3.7 RESIDUAL STRENGTH CALCULATIONS

Program BREAK, another modification of the surface flaw growth analysis routine, was written to make residual strength calculations interactively at a computer terminal. Input consists of K_{IC}, crack depth (a), half crack surface length (c), and thickness and width of the material. Several pairs of a and c values can be input at one time. Residual strength is calculated for the depth and surface locations on the crack front, and the lower of the two is called the residual strength of the crack. The results of these calculations are shown in tables 6 through 10. Only the results for the tool mark type flaw are plotted, because only this one shows significant loss of residual strength (see figure 20).

The tensile yield strength of 7075-T73 forgings is 56 ksi for thicknesses less than three inches according to MIL-HDBK-5. Since the residual strength calculations show strengths in excess of 56 ksi for small crack sizes, the curve has been modified by drawing a line tangent to the curve from the point a=0 and σ=56 ksi. This line defines the residual strength for the smaller crack depths.

Figure 20 also shows a transition from being critical at the depth to being critical at the surface of the crack front. The residual strength degrades at a greater rate from this point. Figure 21 shows a plot of residual strength versus number of landings for the tool mark type flaw.

4.0 CONCLUSIONS

The DTA shows that for a crack in the jack pad fillet area on the underside of the fork, and for the Design/Fatigue Drop Test Spectrum, the nose gear fork has slow crack growth and relatively high residual strength. This analysis does not explain the service failure due to the .024 by .15 inch fatigue crack. It should be noted that the failed fork also had some shallow tool mark induced cracks adjacent to the other crack. The analysis shows that tool mark type cracks give the most rapid crack growth and degradation of residual strength of the five flaw types analyzed. (The tool mark induced crack in combination with the other crack may have resulted in a greater loss of residual strength than either crack by itself, which may explain the failure.) However, the DTA still shows relatively high residual strengths and long crack growth lives for tool mark induced cracks when subjected to the Design/Fatigue Drop Test Spectrum. It appears, therefore, that the short field landings must be producing critical area stresses well in excess of the maximum spectrum stress of 28 ksi. This would mean both greater degradation of residual strength and more rapid crack growth rates. The critical crack size for the tool mark induced crack at the maximum spectrum stress is about .18 inch deep and .80 inch long. Increasing the maximum stress to 42 ksi reduces the critical crack size to .087 inch deep and .548 inch long.

5.0 RECOMMENDATIONS

In view of the fact that no similar failures have occurred since the restriction on short field landings was imposed, we recommend that the restriction be continued. Also, landing procedures where a high potential exists for the nose gear to touch down first should be avoided, since this condition produces the highest stress in the fork. Since tool mark induced flaws in the jack point fillet area are the most critical, care should be taken to avoid tool marks in this area, especially those parallel to the fillet. This area should be polished to remove tool marks.

If the using command decides that short field landings are necessary, the analysis should be updated to reflect the usage. This would require instrumented landing tests to determine loads due to short field landings, crack growth tests to supplement the very limited crack growth rate data available for 7075-T73 forgings, a strain survey of an OV-10A nose landing gear fork to verify the finite element stress analysis, and fracture toughness testing of specimens representative of the critical location.

REFERENCES:

1. Riojas, M. and Morales, A., "Metallurgical Analysis of OV-10A Nose Gear Fork," Lab Control Number 364, SA-ALC/MANCE, Kelly AFB, TX, 13 August 1980.

2. Dill, H.D. and Saff, C.R., "Environment-Load Interaction Effects on Crack Growth," AFFDL-TR-78-137, November 1978.

3. Ferguson, R.R. and Berryman, R.C., "Fracture Mechanics Evaluation of B-1 Materials," AFML-TR-76-137, Vols I and II, October 1976.

4. "Damage Tolerant Design Handbook," MCIC-HB-01, Parts 1 and 2, Metals and Ceramics Information Center, Battelle, Columbus Laboratories, January 1975.

5. "Test Plan Report of Fatigue Tests for the OV-10A Airplane," NA65H-86, 30 Nov 65.

6. "Demonstration Data Report, Structural Demonstration Tests," NA67H-110, Section 2, Parts 1 and 2, 15 December 1968.

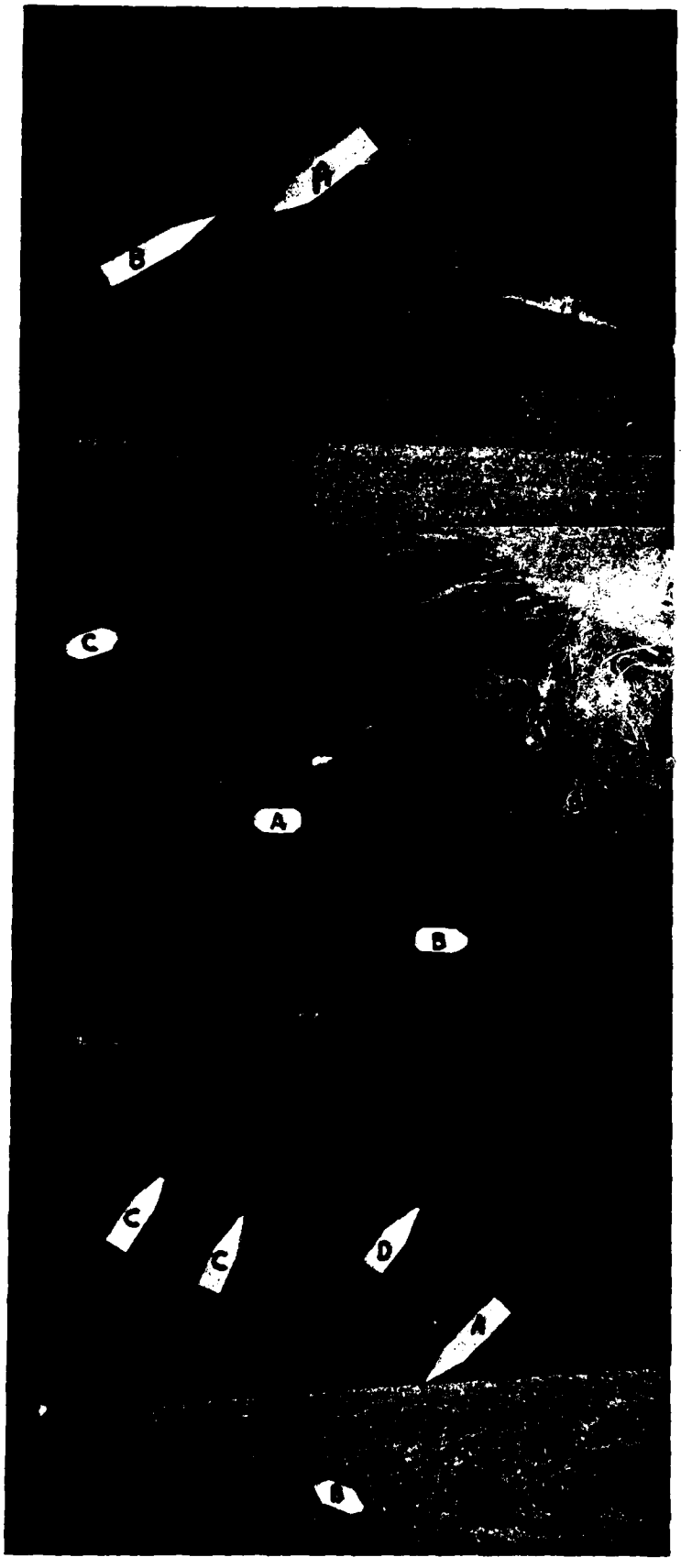

FIGURE 1. OV-10A Nose Gear Failure
A. Primary fatigue crack location
B. Tool mark fatigue crack location

FIGURE 2. Primary Crack 26X
A. Fatigue
B. Fractured surface
C. Machined surface

FIGURE 3. Tool Mark Crack 21X
A. Tool mark induced fatigue crack
B. Fractured surface
C. Secondary cracking
D. Tool mark

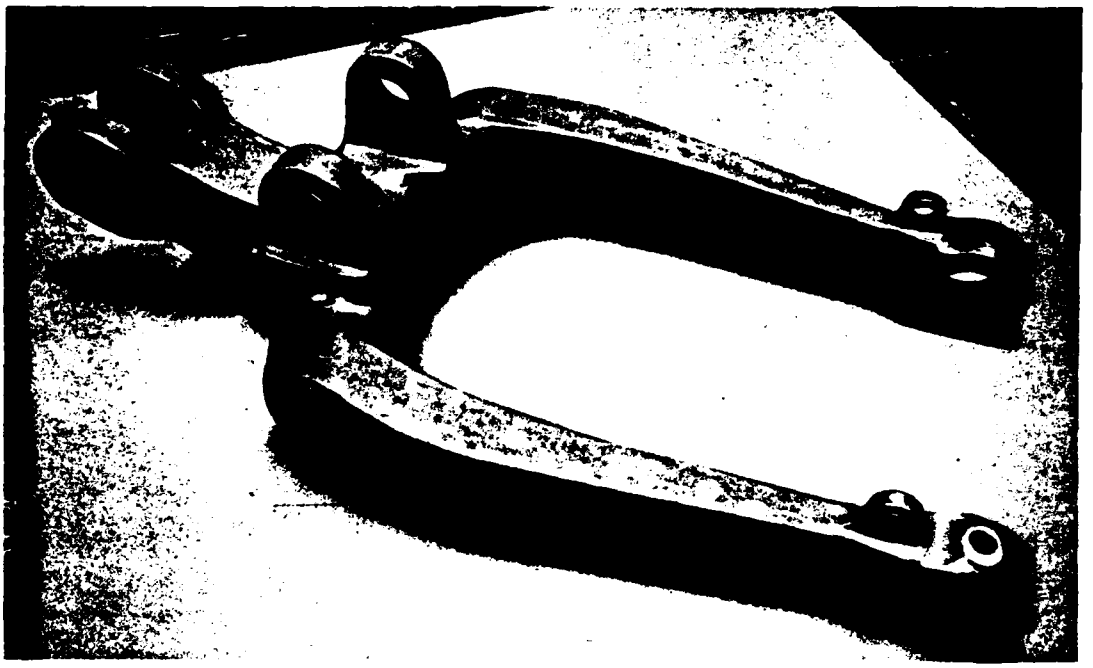

FIGURE 4. OV-10A Nose Gear Fork, Top

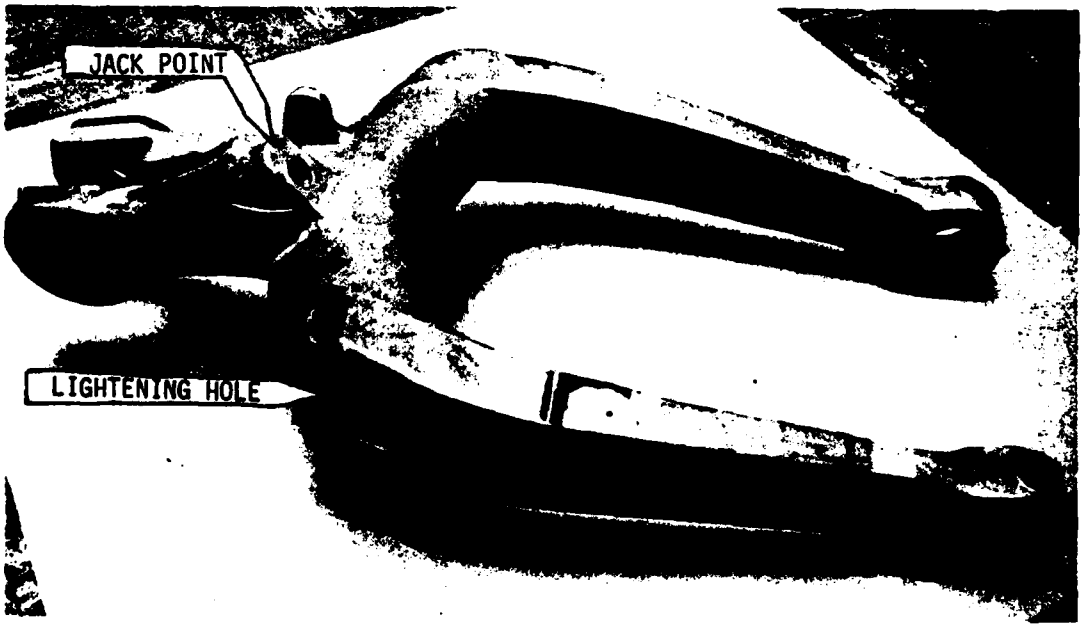

FIGURE 5. OV-10A Nose Gear Fork, Bottom

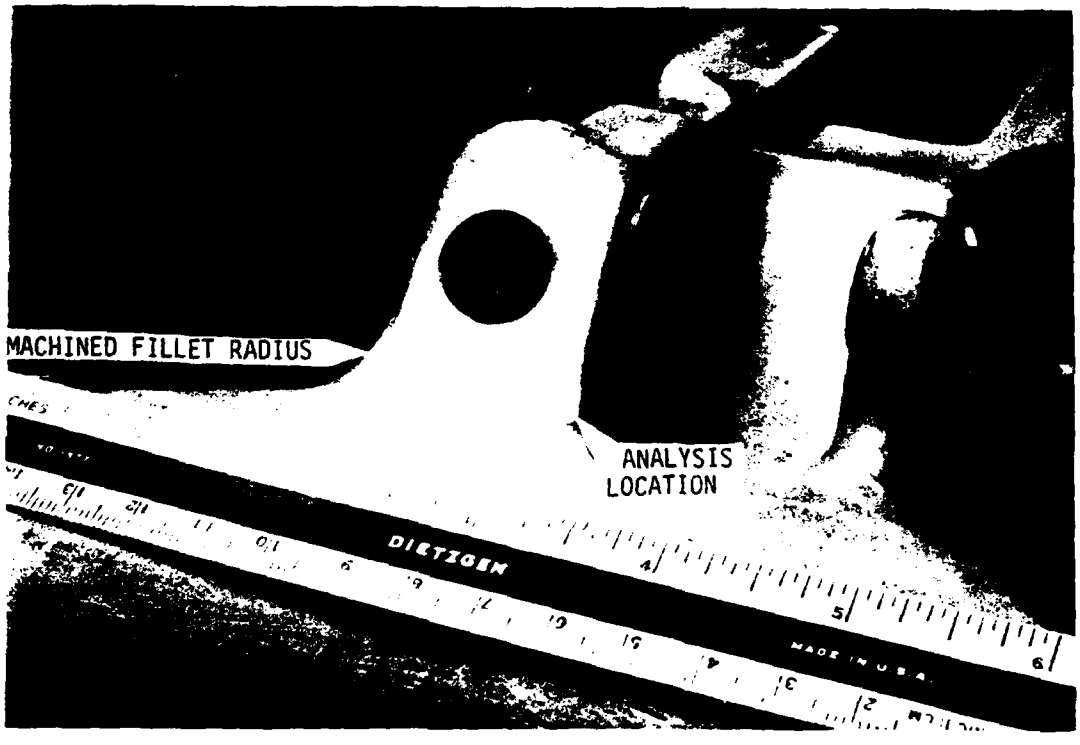

FIGURE 6. Analysis Location

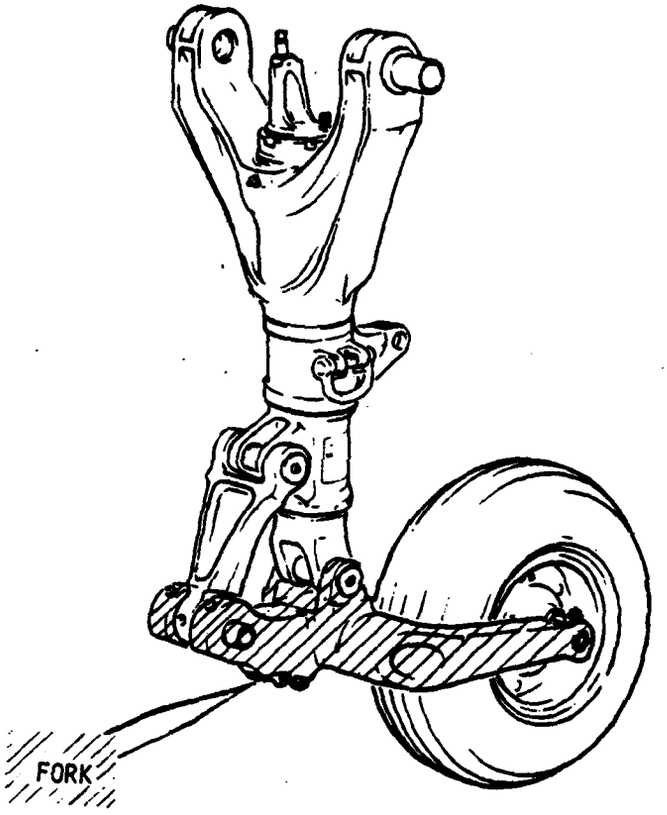

FIGURE 7. OV-10A Nose Gear Assembly

OV-10A NOSE GEAR FORK PERSPECTIVE VIEW

ROTX,ROTY,ROTZ: 0 30 40 PLOT LIMITS: X: -8.80, 14.48 Y: 0.00, 5.94 Z: -2.41, 4.37 DATE: 11/25/81

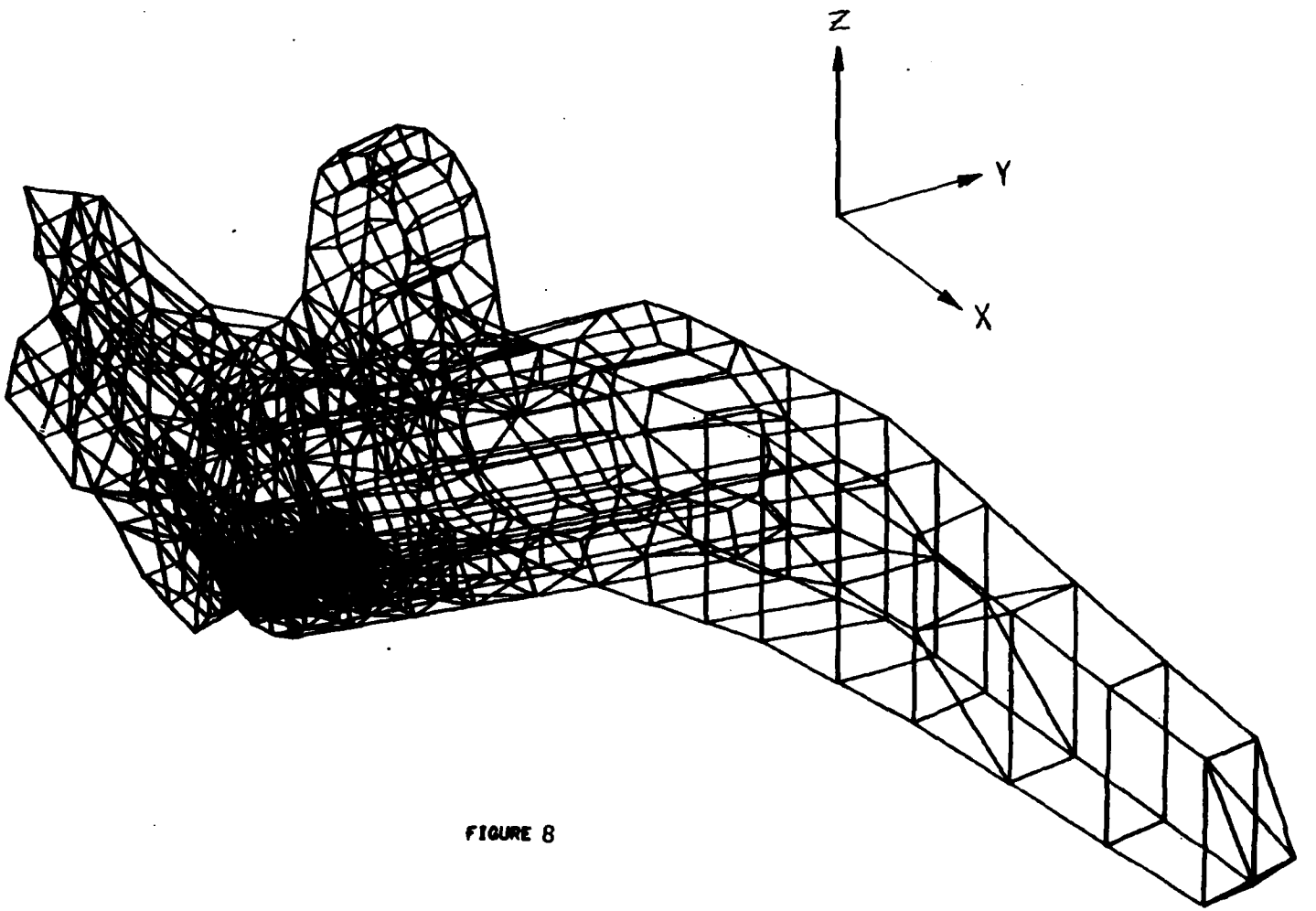

FIGURE 8

OV-10A NOSE GEAR FORK TOP VIEW

ROTX,ROTY,ROTZ: 0 270 90 PLOT LIMITS: X: -6.20, 14.48 Y: 0.00, 5.94 Z: -2.41, 4.37 DATE: 11/25/81

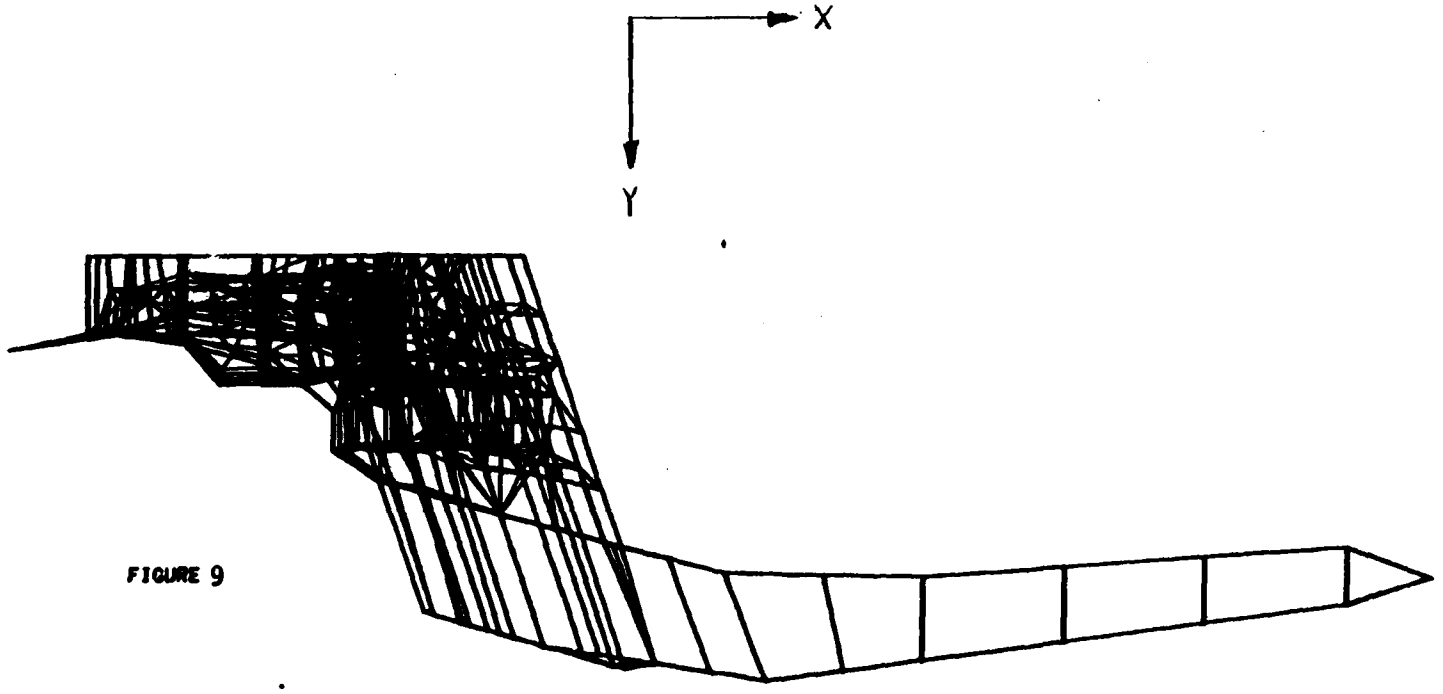

FIGURE 9

OV-10A NOSE GEAR FORK SIDE VIEW

ROTX,ROTY,ROTZ: 0 0 90 PLOT LIMITS: X: -6.20, 14.48 Y: 0.00, 5.94 Z: -2.41, 4.37 DATE: 11/25/81

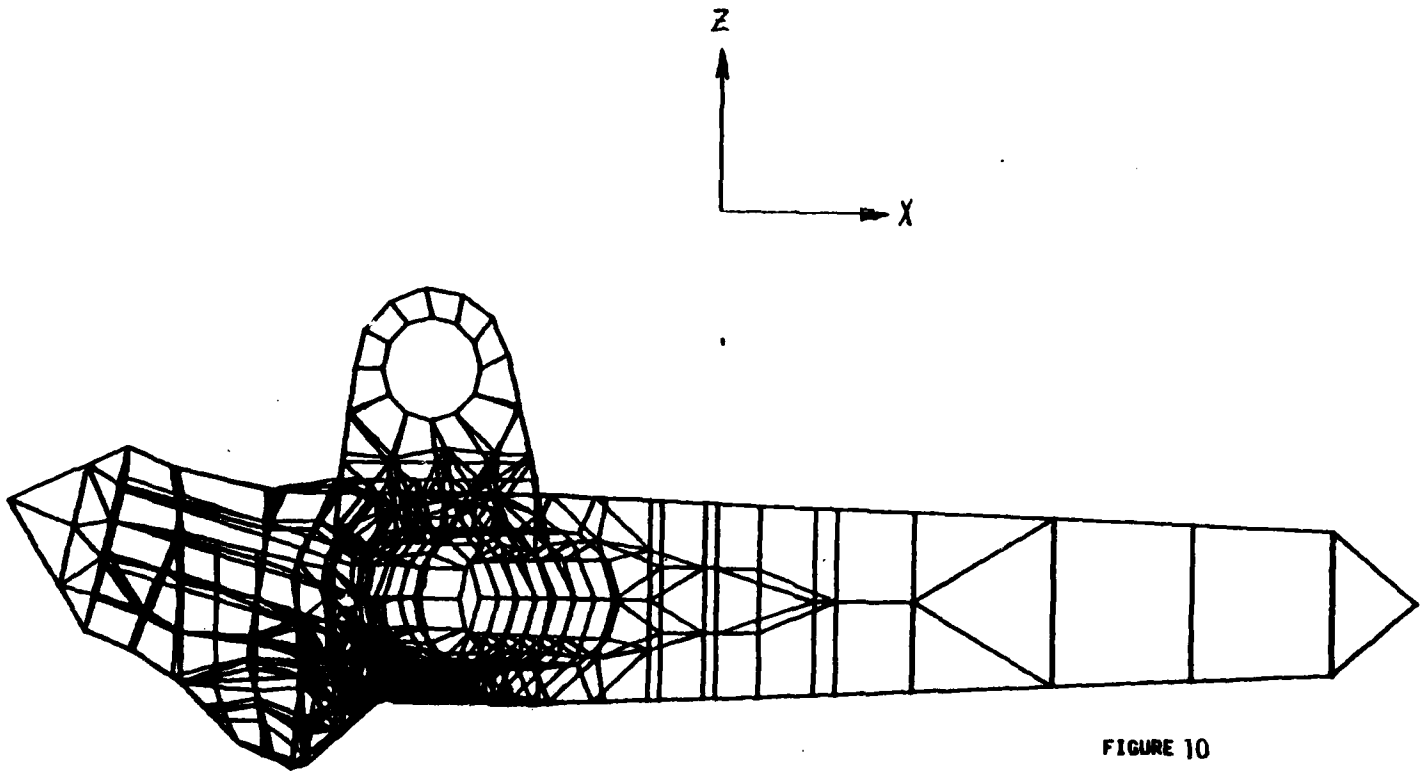

FIGURE 10

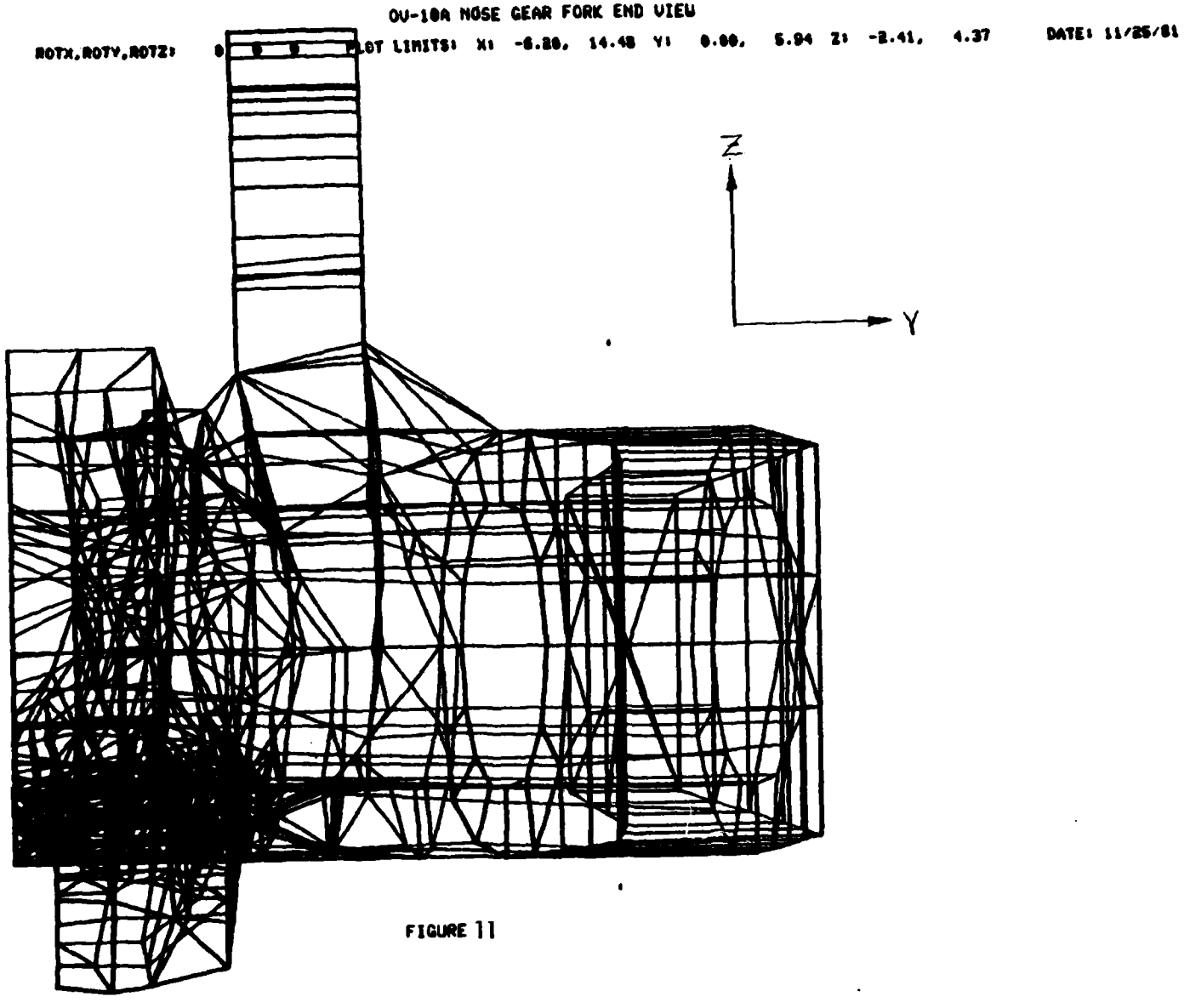
OV-10A NOSE GEAR FORK END VIEW
ROTX,ROTY,ROTZ: 0 0 0
PLOT LIMITS: X: -6.80, 14.48 Y: 0.00, 5.94 Z: -2.41, 4.37
DATE: 11/25/81
Z
Y

FIGURE 11

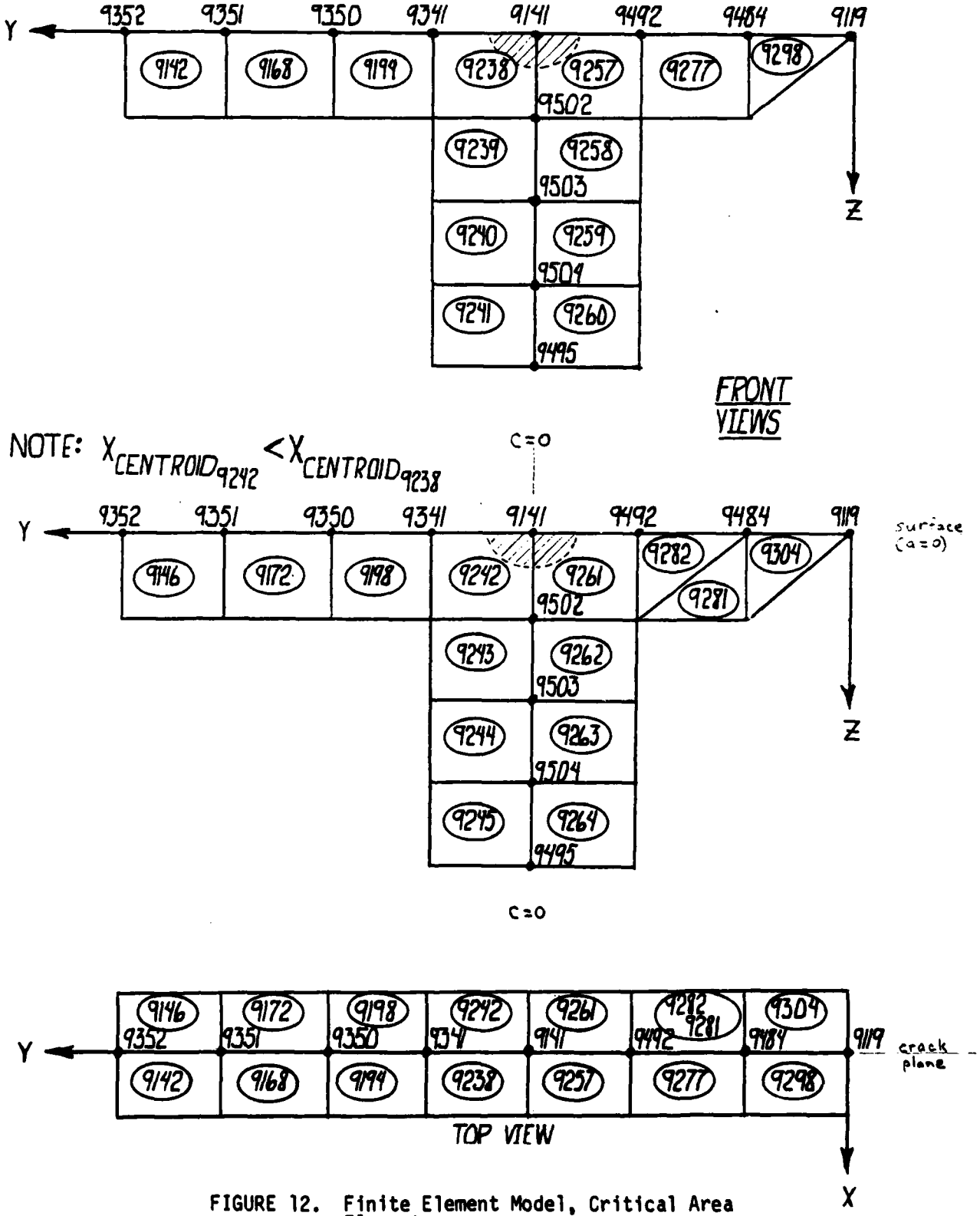

FIGURE 12. Finite Element Model, Critical Area Elements

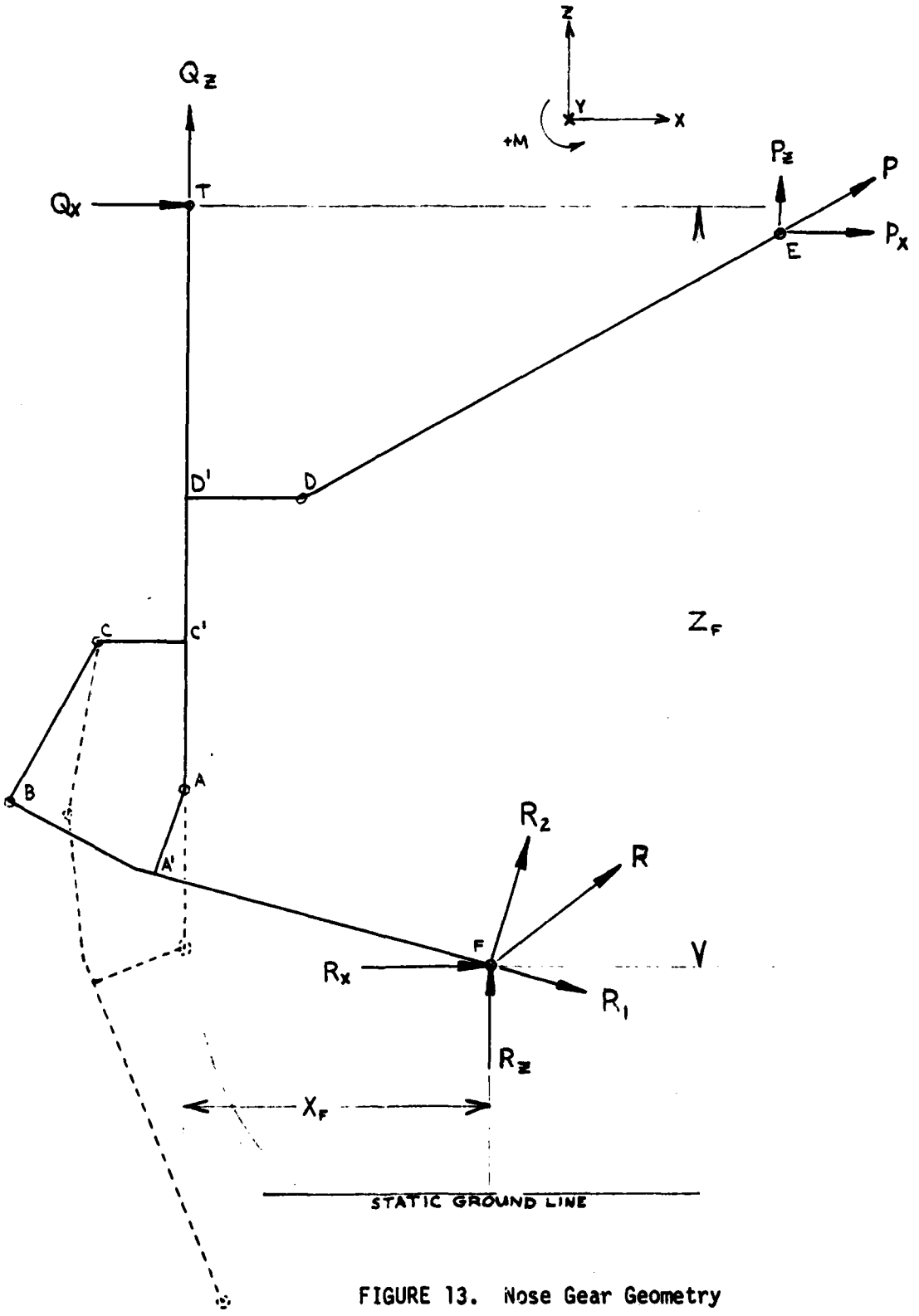

FIGURE 13. Nose Gear Geometry

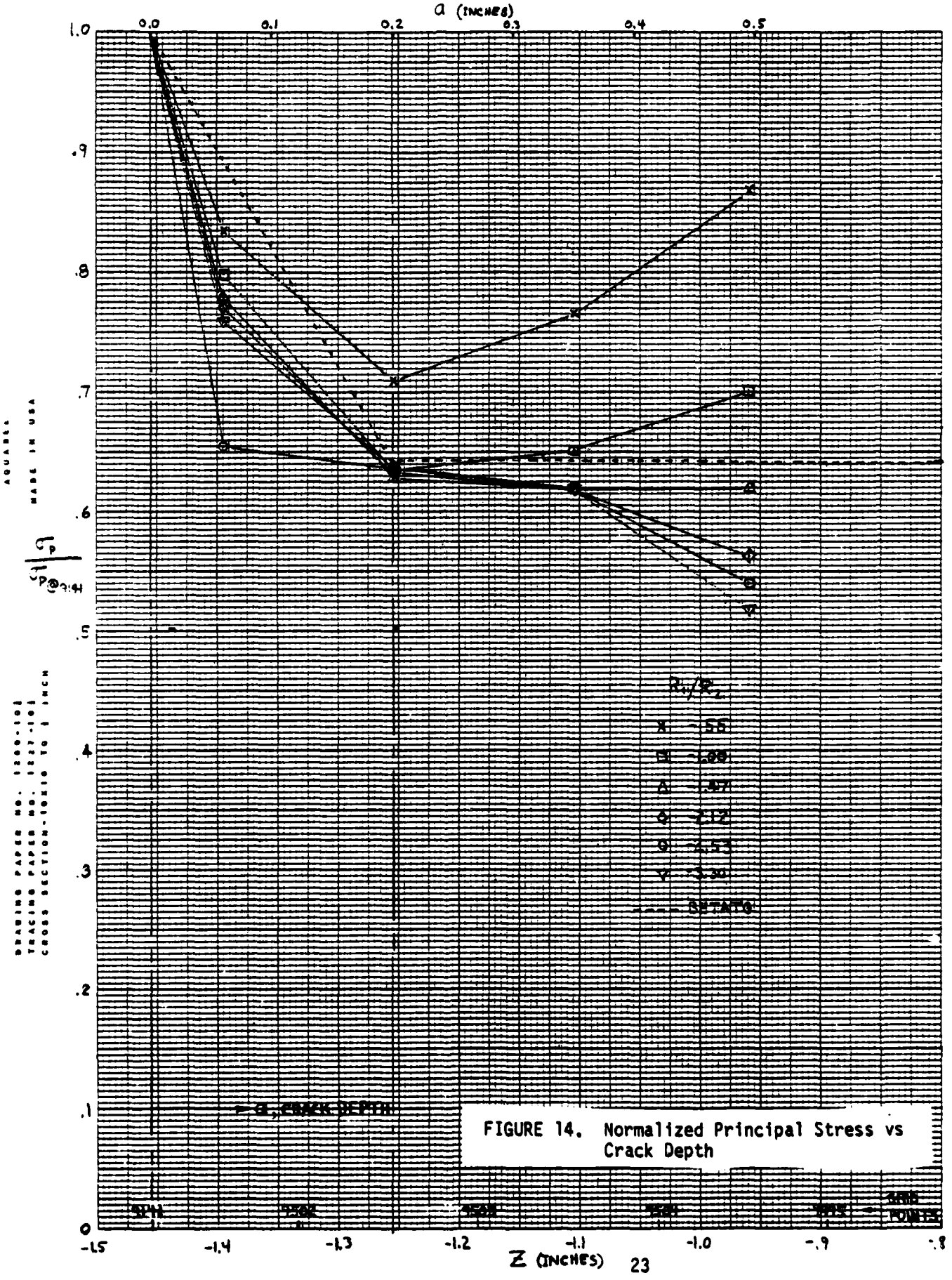

FIGURE 14. Normalized Principal Stress vs Crack Depth

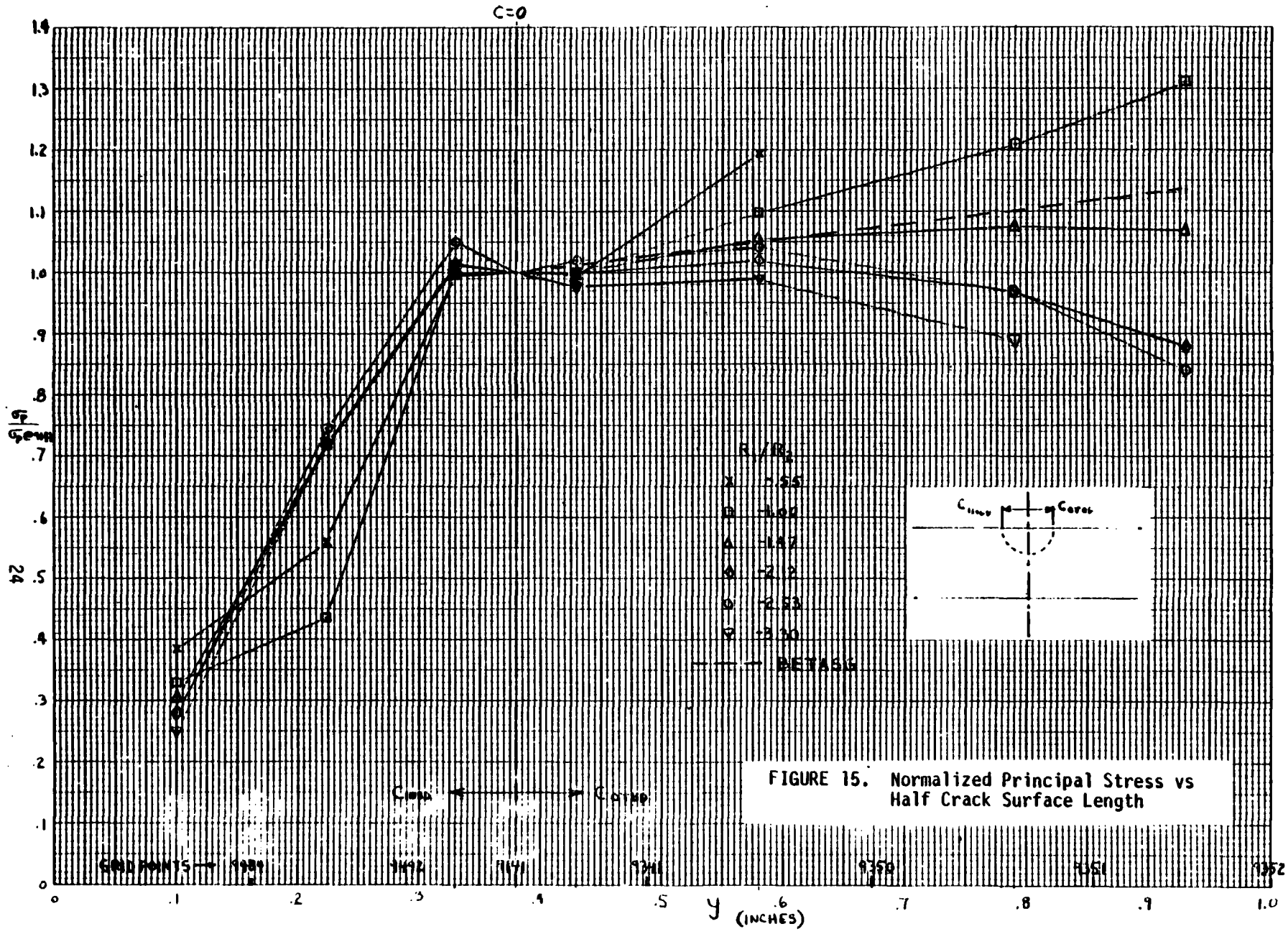

FIGURE 15. Normalized Principal Stress vs Half Crack Surface Length

FIGURE 16. Landing Loads Oscillograph Trace

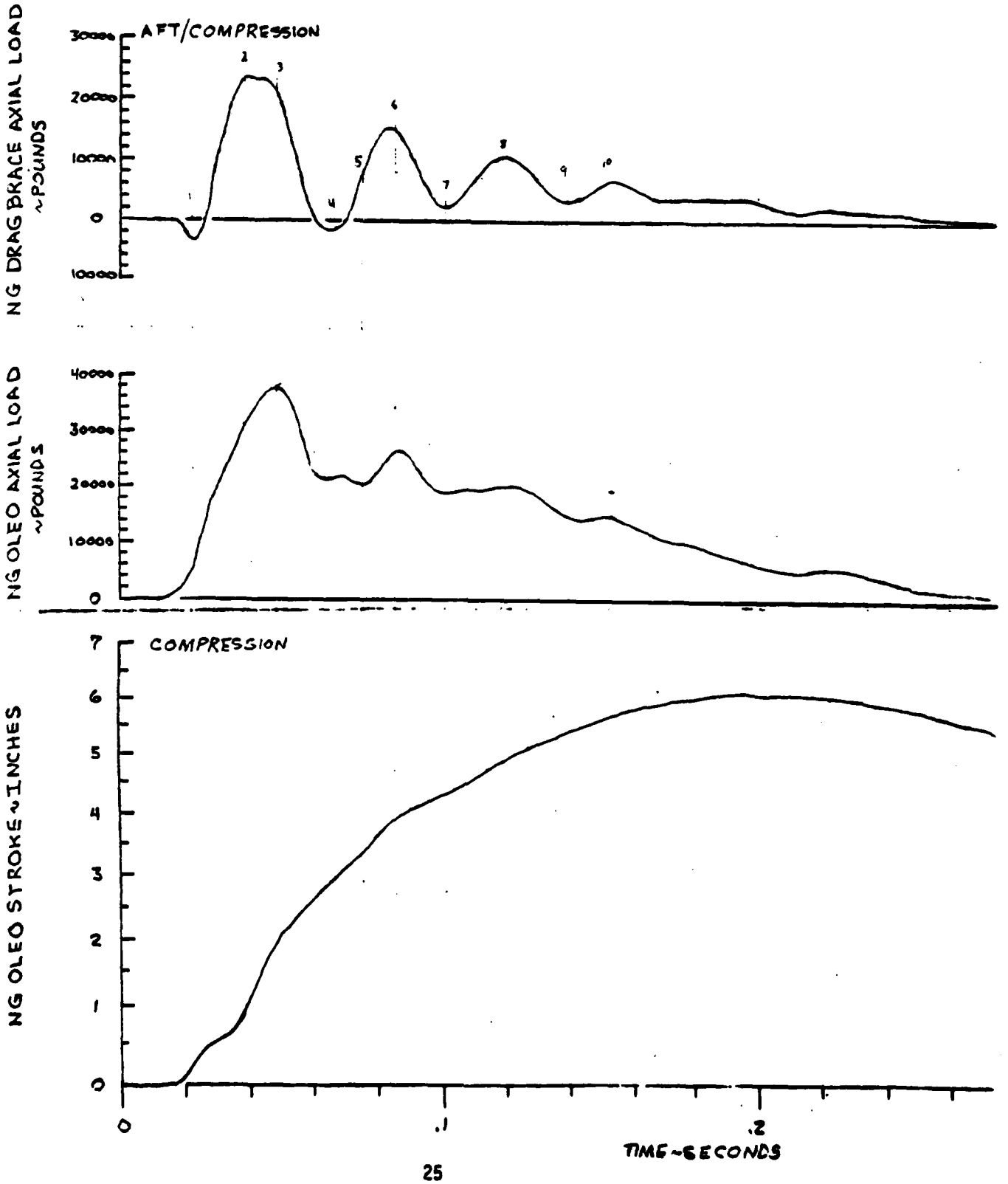

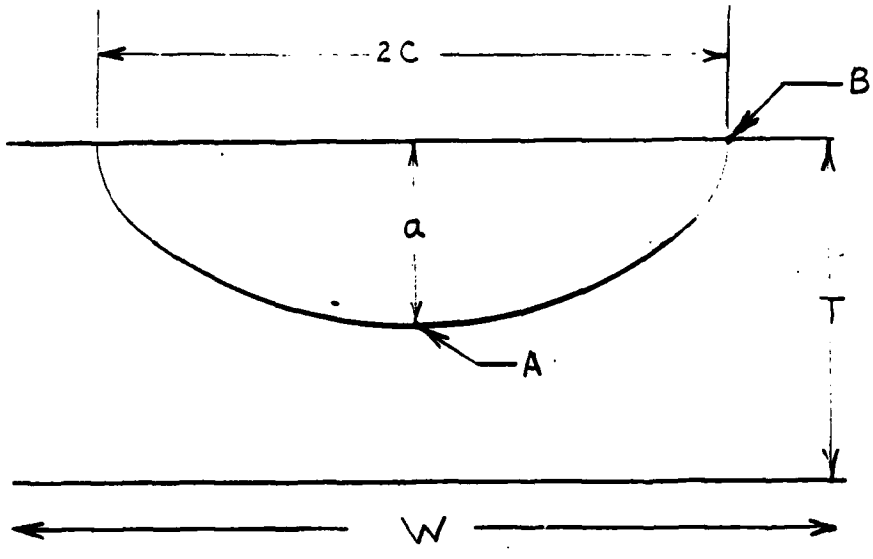

FIGURE 17. Crack Geometry

FIGURE 18. Crack Depth vs Blocks

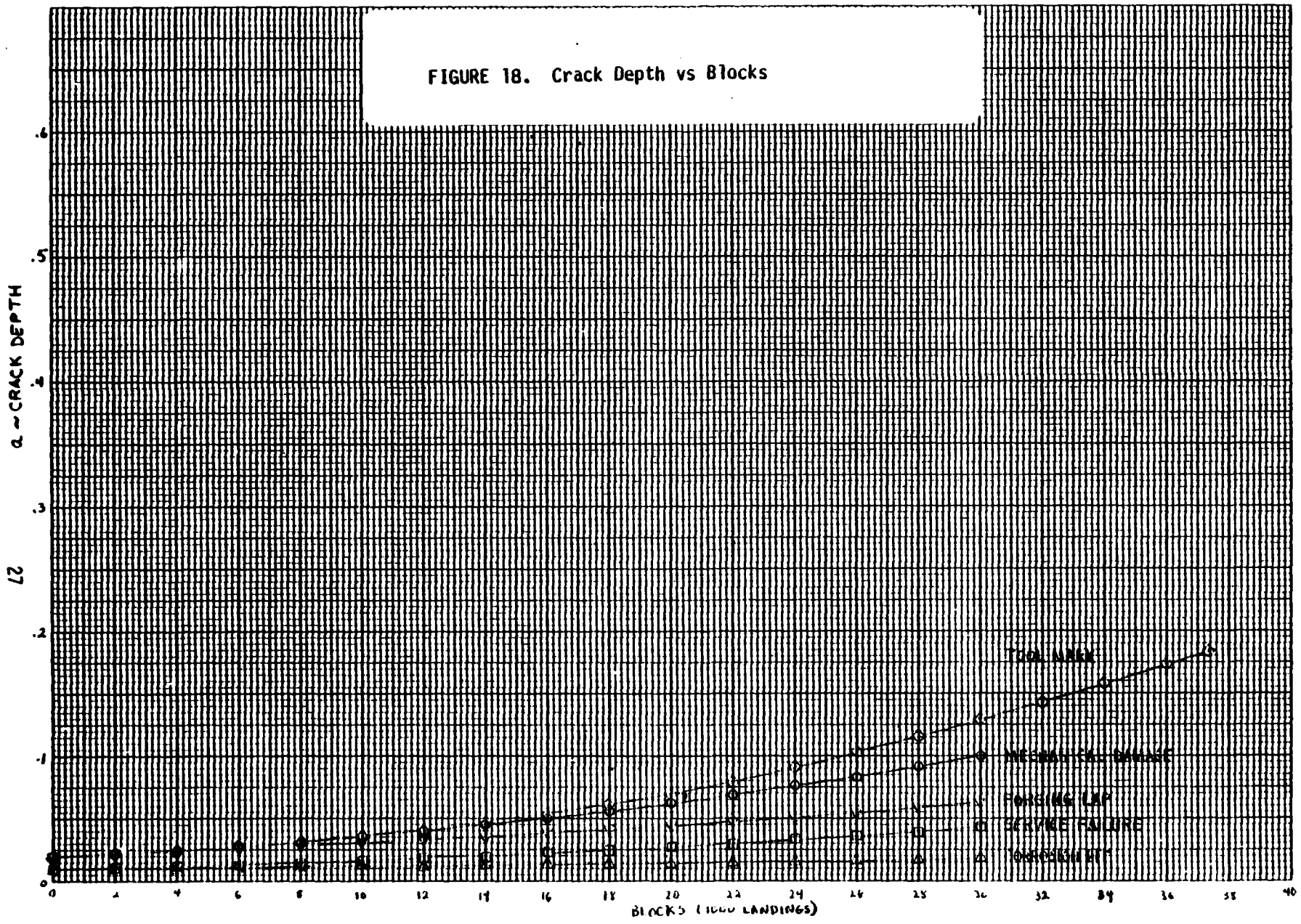

FIGURE 19. Half Crack Surface Length vs Blocks

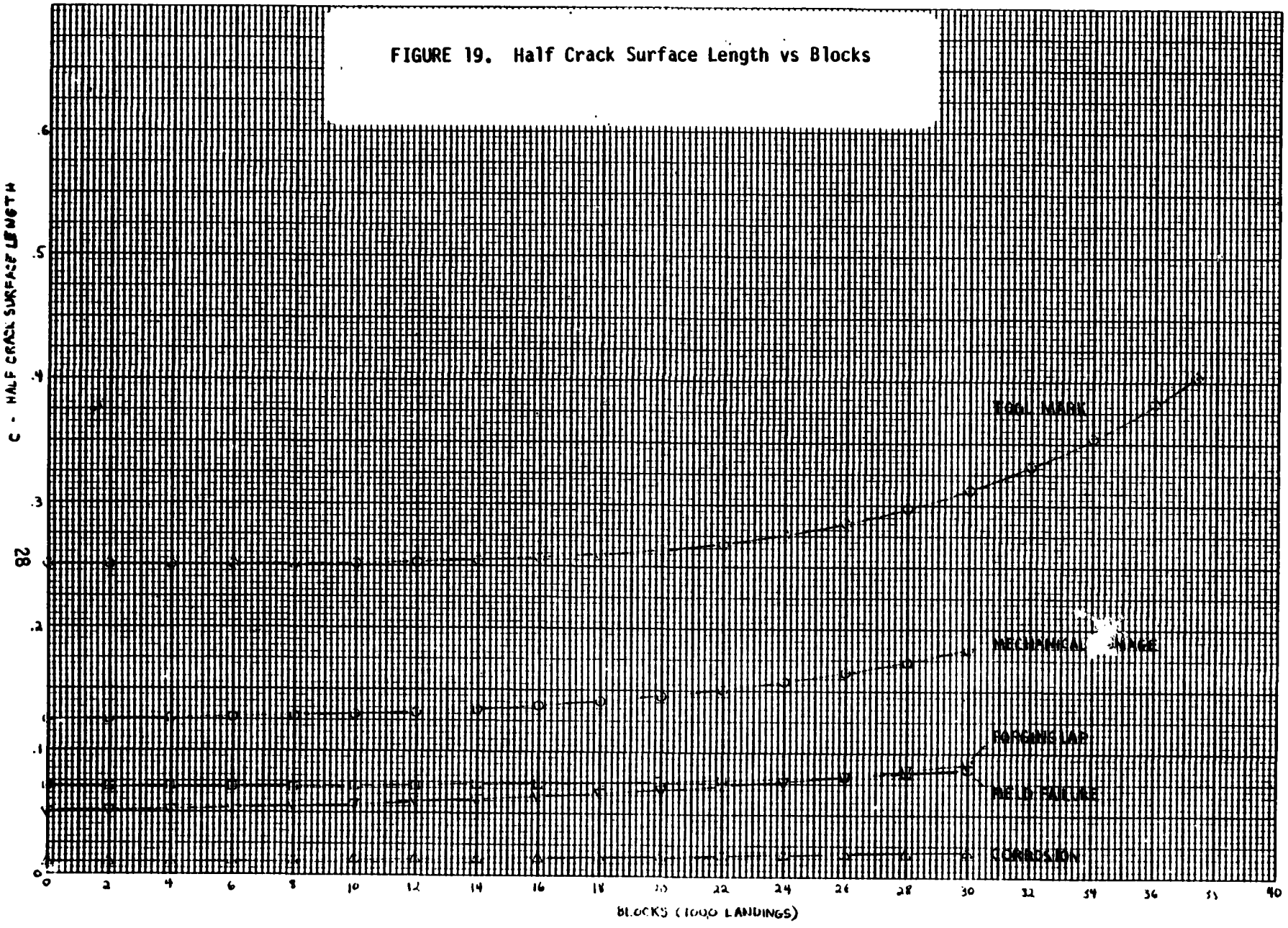

FIGURE 20. Residual Strength vs Crack Depth

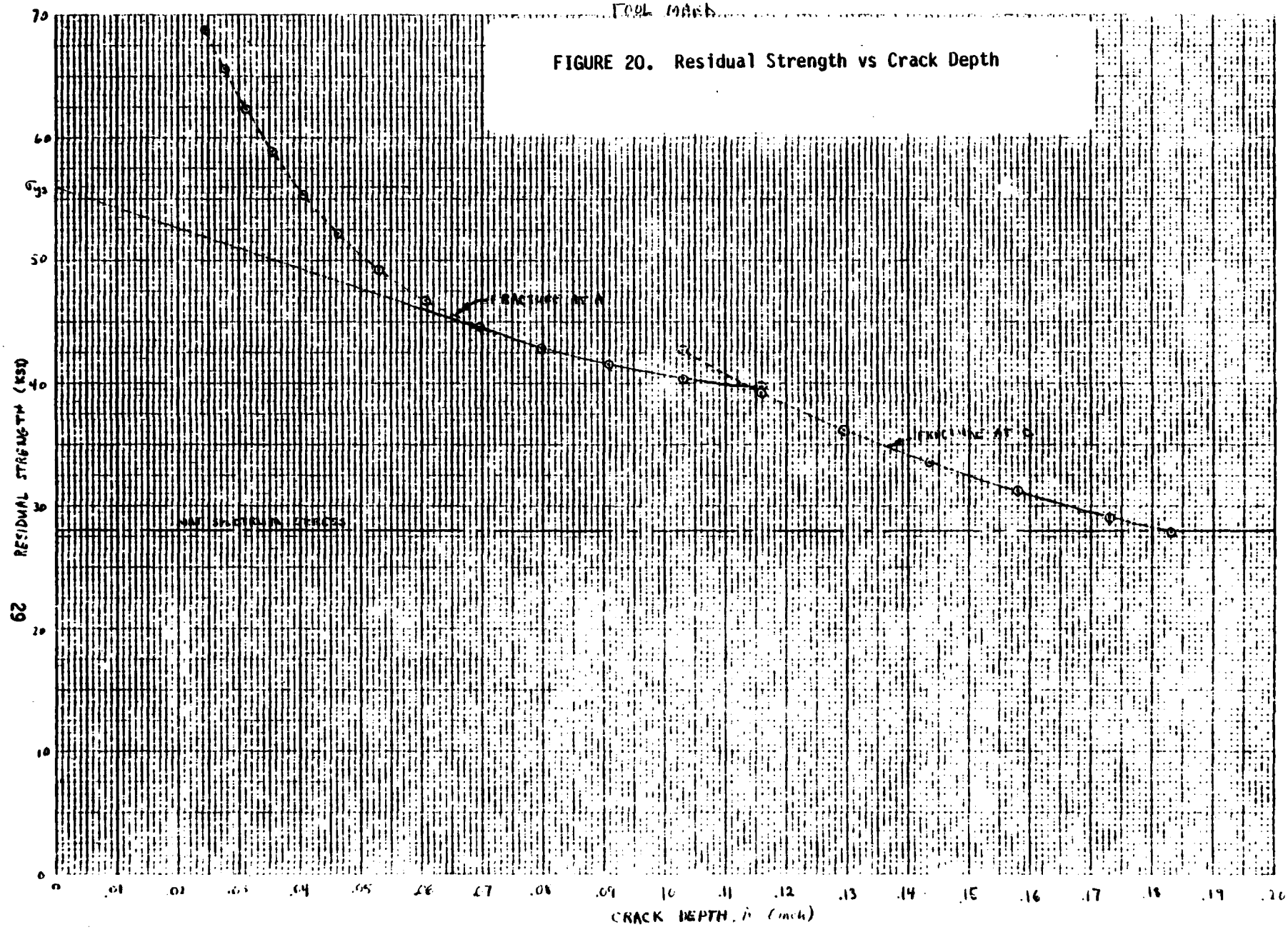

TOOL MARK

FIGURE 21. Residual Strength vs Blocks

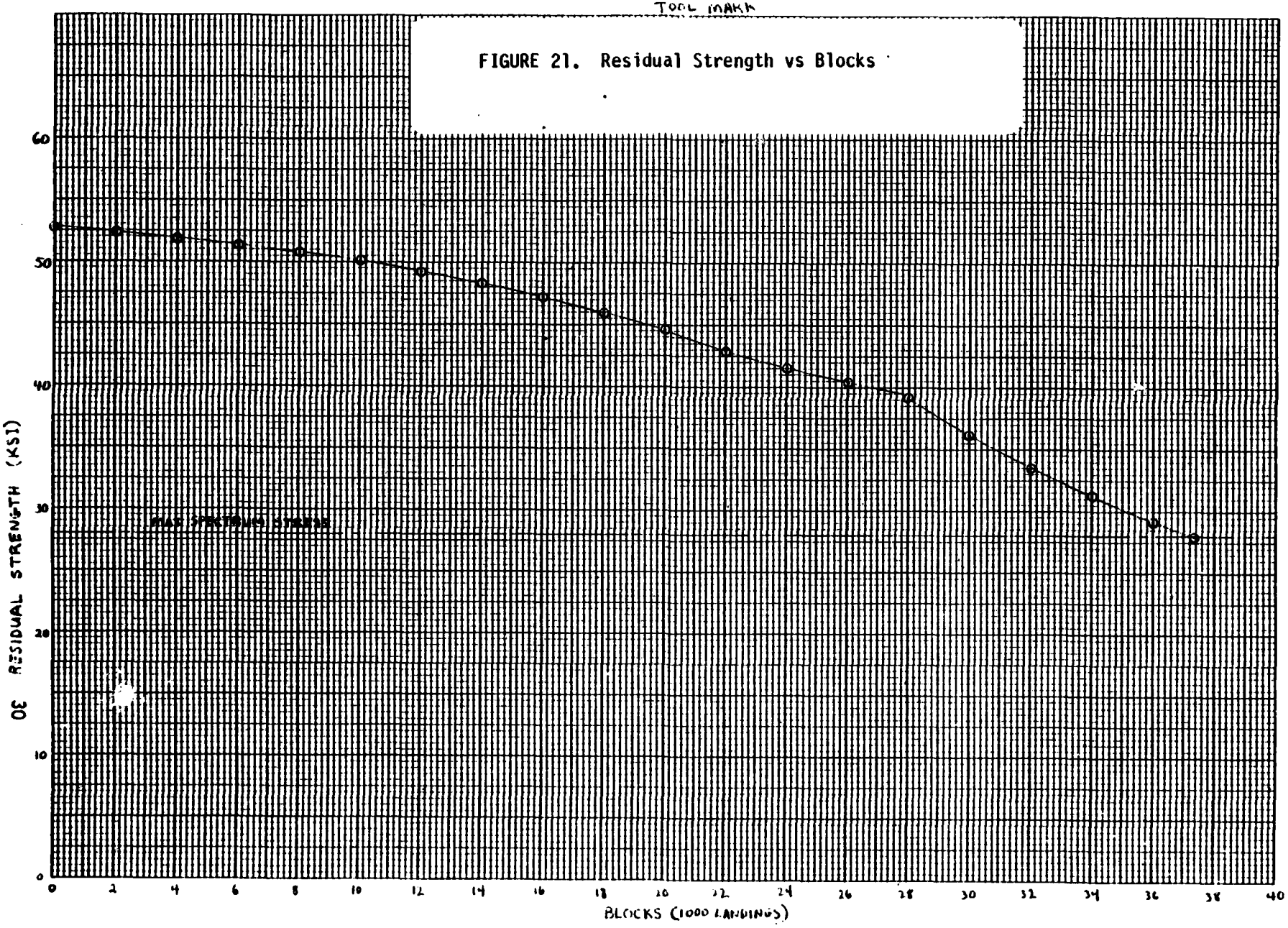

TABLE 1

Stresses (psi) Due to Unit Load (1 lb) in X Direction

Element	σ_x	σ_y	σ_z	τ_{xy}	τ_{yz}	τ_{zx}
9142	-.1269	.0233	-.0077	.0491	-.0151	-.0241
9146	-.1448	-.0022	-.0153	.0329	-.0122	-.0339
9168	-.1898	.0353	-.0131	.0421	-.0130	-.0329
9172	-.2171	.0107	-.0251	.0265	-.0132	-.0510
9194	-.2269	.0481	-.0163	.0440	-.0111	-.0445
9198	-.2648	.0256	-.0373	.0287	-.0091	-.0641
9238	-.2375	.0645	-.0179	.0594	-.0132	-.0504
9239	-.2290	.0633	-.0174	.0373	-.0023	-.0771
9240	-.2342	.0500	-.0037	.0322	-.0038	-.0353
9241	-.1785	.0686	-.0123	.0093	.0073	-.0265
9242	-.2568	.0409	-.0430	.0409	-.0109	-.0739
9243	-.1938	.0657	-.0109	.0325	-.0041	-.0641
9244	-.2193	.0093	-.0041	.0262	-.0057	-.0212
9245	-.1238	.0909	-.0061	.0113	.0111	.0273
9257	-.2376	.0782	-.0137	.0751	-.0137	-.0556
9258	-.2417	.0615	-.0248	.0592	.0063	-.0839
9259	-.2381	.0569	0.0	.0373	-.0011	-.0429
9260	-.2010	.0649	-.0186	.0191	.0003	.0236
9261	-.2712	.0409	-.0445	.0783	-.0038	-.0905
9262	-.1902	.0716	-.0121	.0615	-.0041	-.0717
9263	-.2153	.0603	-.0021	.0408	-.0060	-.0293
9264	-.1377	.0895	-.0135	.0274	.0039	.0261
9277	-.1167	.0900	.0106	.0995	-.0248	-.0559
9281	-.1175	.0868	-.0076	.1101	-.0139	-.0384
9282	-.2259	.0575	-.0088	.1285	-.0329	-.0784
9298	.0180	.1169	.0589	.0359	-.0375	-.0805
9304	-.0425	.1212	.1211	.0491	-.0779	-.0910

TABLE 2

Stresses (psi) Due to Unit Load (1 lb) in Z Direction

Element	σ_x	σ_y	σ_z	τ_{xy}	τ_{yz}	τ_{zx}
9142	.3247	.3713	.0306	.2327	-.0427	-.0447
9146	.3183	.3148	.0338	.2255	-.0132	-.0204
9168	.2827	.3267	.0220	.1644	-.0369	-.0323
9172	.2885	.2847	.0315	.1557	-.0199	-.0089
9194	.2346	.2873	.0163	.1046	-.0423	-.0273
9198	.2410	.2637	.0353	.0821	-.0377	-.0036
9238	.2021	.2741	.0184	.0653	-.0497	-.0255
9239	.1389	.2511	.0368	.0654	-.0679	-.0391
9240	.1184	.2075	.0297	.0827	-.0805	-.0564
9241	.1421	.1381	.0303	.1023	-.0701	-.0727
9242	.1995	.2555	.0509	.0338	-.0661	-.0024
9243	.1536	.2434	.0458	.0485	-.0783	-.0448
9244	.1283	.1761	.0085	.0727	-.0866	-.0547
9245	.1477	.1053	.0247	.1042	-.0720	-.0725
9257	.1551	.2382	.0221	.0567	-.0643	-.0175
9258	.1101	.2523	.0627	.0623	-.0892	-.0463
9259	.1021	.2244	.0293	.0643	-.0922	-.0685
9260	.1575	.1603	.0360	.0779	-.0640	-.0731
9261	.1164	.1887	-.0494	.0675	-.0850	-.0320
9262	.1017	.1987	.0457	.0381	-.1123	-.0419
9263	.1257	.1937	.0100	.0398	-.1277	-.0473
9264	.1865	.1314	.0453	.0802	-.0786	-.0606
9277	.1519	.2803	.0618	.0501	-.1027	-.0556
9281	.0085	.2043	-.0573	.0335	-.1546	-.0936
9282	.1402	.3383	.0929	.0085	-.2116	-.0441
9298	.1562	.1972	.1150	.0542	-.0875	-.1285
9304	.1599	.2591	.3687	.0660	-.2036	-.1173

TABLE 3

LEVEL TERRAIN LANDINGS (561 LANDINGS)

PEAKS		VALLEYS	
STRESS	OCCURRENCES	STRESS	OCCURRENCES
21000	94	8000	2
20000	61	7000	26
19000	52	6000	58
18000	52	5000	100
17000	54	4000	158
16000	57	3000	240
15000	49	2000	358
14000	86	1000	554
13000	75	0	504
12000	85		
11000	85		
10000	100		
9000	110		
8000	90		
7000	120		
6000	130		
5000	140		
4000	160		
3000	170		
2000	230		

TABLE 4

TYPE A ROUGH TERRAIN LANDINGS (106 LANDINGS)

PEAKS		VALLEYS	
STRESS	OCCURRENCES	STRESS	OCCURRENCES
28000	3	11000	1
27000	5	10000	4
26000	6	9000	6
25000	8	8000	9
24000	11	7000	15
23000	10	6000	18
22000	16	5000	21
21000	14	4000	27
20000	13	3000	38
19000	14	2000	57
18000	15	1000	90
17000	15	0	161
16000	20	-1000	83
15000	17	-2000	41
14000	20	-3000	16
13000	20	-4000	3
12000	23		
11000	20		
10000	21		
9000	29		
8000	20		
7000	40		
6000	20		
5000	45		
4000	45		
3000	50		
2000	70		

TABLE 5

TYPES B AND C ROUGH TERRAIN LANDINGS (333 LANDINGS)

PEAKS		VALLEYS	
STRESS	OCCURRENCES	STRESS	OCCURRENCES
27000	10	11000	6
26000	16	10000	12
25000	24	9000	20
24000	22	8000	25
23000	28	7000	36
22000	23	6000	46
21000	27	5000	51
20000	30	4000	88
19000	35	3000	119
18000	35	2000	195
17000	45	1000	404
16000	44	0	396
15000	51	-1000	160
14000	50	-2000	51
13000	60	-3000	25
12000	60	-4000	12
11000	70	-5000	4
10000	70		
9000	70		
8000	75		
7000	85		
6000	90		
5000	130		
4000	120		
3000	180		
2000	200		

TABLE 6

```
*ENTER KSUBC*      SERVICE FAILURE
19
*ENTER NO. OF CRACK SIZES EACH OF A AND C*
16
*ENTER VALUES OF A*
.0100 .0110 .0121 .0134 .0148 .0163 .0181 .0200 .0222 .0245 .0271 .0299 .0329 .0361 .0396 .0433

*ENTER VALUES OF C*
.0705 .0707 .0709 .0711 .0715 .0719 .0725 .0732 .0741 .0751 .0764 .0780 .0798 .0819 .0844 .0872

*ENTER THICKNESS AND WIDTH*
.5 5.88
      A        BETAA     BETATG      SIGA         C        BETAB     BETASQ       SIGB         A       SIGRES
    .0100     1.0184     .9821    107.17     .0705     .1725     1.0177    229.84     .0100    107.17
    .0110     1.0160     .9803    102.61     .0707     .1987     1.0178    205.54     .0110    102.61
    .0121     1.0138     .9784     98.25     .0709     .2140     1.0178    184.73     .0121     98.25
    .0134     1.0108     .9760     93.06     .0711     .2382     1.0179    165.74     .0134     93.06
    .0148     1.0078     .9735     89.08     .0715     .2621     1.0180    150.20     .0148     89.08
    .0163     1.0019     .9709     86.31     .0719     .2861     1.0181    137.19     .0163     86.31
    .0181      .9948     .9678     82.76     .0725     .3124     1.0182    125.09     .0181     82.76
    .0200      .9866     .9642     79.67     .0732     .3378     1.0184    115.14     .0200     79.67
    .0222      .9764     .9603     76.73     .0741     .3643     1.0186    106.09     .0222     76.73
    .0245      .9654     .9562     74.19     .0751     .3893     1.0188     98.58     .0245     74.19
    .0271      .9531     .9516     71.80     .0764     .4144     1.0192     91.78     .0271     71.80
    .0299      .9405     .9466     69.64     .0780     .4381     1.0196     85.89     .0299     69.64
    .0329      .9276     .9412     67.69     .0798     .4607     1.0201     80.71     .0329     67.69
    .0361      .9148     .9355     65.92     .0819     .4818     1.0208     76.13     .0361     65.92
    .0396      .9024     .9292     64.24     .0844     .5019     1.0218     71.95     .0396     64.24
    .0433      .8905     .9226     62.70     .0872     .5204     1.0219     68.22     .0433     62.70
*JOB DONE*
     END  BREAK
      .283 CP SECONDS EXECUTION TIME
..
```

TABLE 7

MECHANICAL DAMAGE

```
*ENTER KSUBC*
10
*ENTER NO. OF CRACK SIZES EACH OF A AND C*
16
*ENTER VALUES OF A*
.020 .0224 .0251 .0282 .0317 .0356 .0400 .0448 .0502 .0560 .0622 .0689 .0780 .0835 .0915 .1000

*ENTER VALUES OF C*
.125 .1255 .1262 .1270 .1282 .1298 .1317 .1342 .1373 .1410 .1456 .1510 .1575 .1650 .1739 .1841

*ENTER THICKNESS AND WIDTH*
.5 500
    .88
      A        BETAA     BETATG     SIGA        C        BETAB     BETASG     SIGB        A       SIGRES

    .0200     1.0195      .9642    77.10      .1250      .1989     1.0314   147.61     .0200     77.10
    .0224     1.0187      .9600    73.24      .1255      .2048     1.0316   130.33     .0224     73.24
    .0251     1.0188      .9551    69.67      .1262      .2520     1.0317   115.94     .0251     69.67
    .0282     1.0130      .9496    66.36      .1270      .2809     1.0319   103.64     .0282     66.36
    .0317     1.0072      .9433    63.37      .1282      .3104     1.0322    93.32     .0317     63.37
    .0356      .9993      .9364    60.72      .1298      .3399     1.0326    84.68     .0356     60.72
    .0400      .9892      .9285    58.36      .1317      .3698     1.0331    77.23     .0400     58.36
    .0448      .9778      .9199    56.30      .1342      .3983     1.0337    70.98     .0448     56.30
    .0502      .9650      .9103    54.47      .1373      .4266     1.0345    65.48     .0502     54.47
    .0560      .9518      .8999    52.89      .1410      .4529     1.0354    60.70     .0560     52.89
    .0622      .9382      .8888    51.49      .1456      .4768     1.0366    56.76     .0622     51.49
    .0689      .9270      .8768    50.25      .1510      .4989     1.0380    53.18     .0689     50.25
    .0780      .9102      .8641    49.12      .1575      .5184     1.0396    50.03     .0780     49.12
    .0835      .9068      .8507    48.00      .1650      .5356     1.0415    47.21     .0835     47.81
    .0915      .8993      .8364    47.18      .1739      .5506     1.0437    44.64     .0915     44.64
    .1000      .8934      .8212    46.20      .1841      .5634     1.0463    42.28     .1000     42.28
*JOB DONE*
     END  BREAK
       .291 CP SECONDS EXECUTION TIME
..
```

TABLE 8

```
                    CORROSION PIT
*ENTER KSUBC*
1
*ENTER NO. OF CRACK SIZES EACH OF A AND C*
16
*ENTER VALUES OF A*
.01 .0103 .0107 .0111 .0115 .0119 .0124 .0129 .0134 .0139 .0145 .0151 .0157 .0164 .0171 .0178

*ENTER VALUES OF C*
.01 .0105 .0109 .0115 .0120 .0125 .0131 .0137 .0144 .0151 .0158 .0165 .0173 .0182 0191
                                                                                .0191 .0200

*ENTER THICKNESS AND WIDTH*
.5 5.88
      A        BETAA     BETATG      SIGA        C       BETAB     BETASG      SIGB        A       SIGRES
    .0100      .6803      .9821    160.43      .0100     .7499     1.0025    142.59      .0100     142.59

    .0103      .6861      .9816    156.83      .0105     .7432     1.0026    140.40      .0103     140.40
    .0107      .6860      .9809    154.01      .0109     .7434     1.0027    137.73      .0107     137.73
    .0111      .6911      .9802    150.80      .0115     .7378     1.0029    136.14      .0111     136.14

    .0115      .6933      .9794    147.20      .0120     .7351     1.0030    132.72      .0115     138.72
    .0119      .6964      .9787    144.38      .0125     .7328     1.0031    130.42      .0119     130.42
    .0124      .6972      .9778    141.80      .0131     .7308     1.0033    127.72      .0124     127.72
    .0129      .6989      .9769    138.83      .0137     .7291     1.0034    126.18      .0129     126.18
    .0134      .7025      .9760    135.05      .0144     .7250     1.0036    122.76      .0134     122.76
    .0139      .7059      .9751    132.09      .0151     .7213     1.0038    120.48      .0139     120.48
    .0145      .7068      .9741    129.28      .0158     .7203     1.0040    117.92      .0145     117.92
    .0151      .7079      .9730    126.65      .0165     .7194     1.0041    115.52      .0151     115.52
    .0157      .7105      .9719    123.88      .0173     .7165     1.0043    113.24      .0157     113.24
    .0164      .7128      .9707    120.97      .0182     .7142     1.0046    110.75      .0164     110.75
    .0171      .7149      .9694    118.27      .0191     .7120     1.0048    108.42      .0171     108.42
    .0178      .7168      .9682    115.78      .0200     .7100     1.0050    106.22      .0178     106.22
*JOB DONE*
     END  BREAK

      .302 CP SECONDS EXECUTION TIME
..
```

TABLE 9

```
*ENTER KSUBC*          FORGING LAP
10
*ENTER NO. OF CRACK SIZES EACH OF A AND C*
16
*ENTER VALUES OF A*
.02 .0218 .0237 .0257 .0279 .0302 .0326 .0352 .0380 .0409 .0440 .0472 .0507 .0544 .0584 .0626

*ENTER VALUES OF C*
.05 .0511 .0523 .0537 .0552 .0570 .0590 .0612 .0637 .065
                                                    65 .0696 .0730 .0768 .0810 .0856 .0907

*ENTER THICKNESS AND WIDTH*
.5 5.88
      A        BETAA     BETATG     SIGA         C       BETAB     BETASQ     SIGB         A      SIGRES

    .0200      .9252     .9648    84.97      .0500      .4503     1.0126   105.13     .0200     84.97
    .0218      .9129     .9610    82.76      .0511      .4702     1.0128    99.56     .0218     82.76
    .0237      .9008     .9576    80.72      .0523      .4891     1.0131    94.58     .0237     80.72

    .0257      .8894     .9541    78.80      .0537      .5064     1.0136    90.11     .0257     78.80
    .0279      .8776     .9501    76.97      .0552      .5239     1.0139    85.88     .0279     76.97
    .0302      .8670     .9460    75.21      .0570      .5392     1.0143    82.08     .0302     75.21
    .0326      .8574     .9417    73.53      .0590      .5529     1.0148    78.63     .0326     73.53
    .0352      .8480     .9371    71.90      .0612      .5663     1.0154    75.34     .0352     71.90
    .0380      .8384     .9321    70.29      .0637      .5785     1.0160    72.24     .0380     70.29
    .0409      .8321     .9269    68.72      .0665      .5889     1.0167    69.40     .0409     68.72
    .0440      .8256     .9213    67.18      .0696      .5985     1.0175    66.70     .0440     66.70
    .0472      .8204     .9156    65.68      .0730      .6064     1.0184    64.22     .0472     64.22
    .0507      .8156     .9094    64.19      .0768      .6140     1.0193    61.78     .0507     61.78
    .0544      .8118     .9027    62.71      .0810      .6204     1.0204    59.47     .0544     59.47
    .0584      .8085     .8956    61.26      .0856      .6264     1.0215    57.23     .0584     57.23
    .0626      .8063     .8881    59.84      .0907      .6311     1.0228    55.11     .0626     55.11
*JOB DONE*
     END  BREAK

      .295 CP SECONDS EXECUTION TIME
..
```

TABLE 10

```
*ENTER KSUBC*                              TOOL MARK
19
*ENTER NO. OF CRACK SIZES EACH OF A AND C*
16
*ENTER VALUES OF A*
.019 .0217 .0245 .0277 .0313 .0355 .0405 .0462 .0530 .0608 .0698 .0798 .0909 .1030 .1158 .1293

*ENTER VALUES OF C*
.250 .2501 .2503 .2506 .2510 .2517 .2526 .2540 .2560 .2589 .2629 .2683 .2756 .2851 .2972 .3124

*ENTER THICKNESS AND WIDTH*
.5 5.88
```

A	BETAA	BETATG	SIGA	C	BETAB	BETASG	SIGB	A	SIGRES
.0190	1.1129	.9660	72.34	.2500	.0862	1.0629	232.92	.0190	72.34
.0217	1.0651	.9612	71.08	.2501	.0952	1.0629	210.93	.0217	71.08
.0245	1.0421	.9562	68.73	.2503	.1084	1.0629	185.05	.0245	68.73
.0277	1.0319	.9505	65.67	.2506	.1260	1.0630	159.16	.0277	65.67
.0313	1.0300	.9440	62.31	.2510	.1470	1.0631	136.32	.0313	62.31
.0355	1.0328	.9365	58.82	.2517	.1716	1.0633	116.60	.0355	58.82
.0405	1.0375	.9276	55.35	.2526	.2001	1.0635	99.78	.0405	55.35
.0462	1.0418	.9174	52.18	.2540	.2307	1.0639	86.25	.0462	52.18
.0530	1.0443	.9052	49.26	.2560	.2646	1.0644	74.89	.0530	49.26
.0608	1.0436	.8913	46.74	.2589	.2996	1.0651	65.70	.0608	46.74
.0698	1.0394	.8752	44.60	.2629	.3358	1.0661	58.11	.0698	44.60
.0798	1.0321	.8573	42.89	.2683	.3711	1.0675	51.98	.0798	42.89
.0909	1.0226	.8375	41.52	.2756	.4049	1.0693	46.91	.0909	41.52
.1030	1.0122	.8159	40.45	.2851	.4364	1.0717	42.68	.1030	40.45
.1158	1.0025	.7930	39.63	.2972	.4643	1.0747	39.16	.1158	39.16
.1293	.9947	.7688	38.98	.3124	.4883	1.0785	36.16	.1293	36.16

```
*JOB DONE*
     END  BREAK
    021600 MAXIMUM EXECUTION FL.
      .394 CP SECONDS EXECUTION TIME.
..
```

TABLE 10 Continued

```
                    TOOL MARK, CONTINUED
*ENTER KSUBC*
10
*ENTER NO. OF CRACK SIZES EACH OF A AND C*
8
*ENTER VALUES OF A*
.1363 .1434 .1506 .1579 .1654 .1730 .1807 .1830
*ENTER VALUES OF C*
.3214 .3312 .3423 .3545 .3680 .3828 .3982 .4043
*ENTER THICKNESS AND WIDTH*
.5 5.88
      A        BETAA      BETATG      SIGA         C        BETAB      BETASQ      SIGB         A       SIGMES
    .1363      .9919       .7663     38.70       .3214      .4989     1.0008     34.81      .1363      34.81

    .1434      .9900       .7436     38.45       .3313      .5083     1.0033     33.55      .1434      33.55
    .1506      .9898       .7308     38.21       .3423      .5187     1.0051     32.38      .1506      38.38
    .1579      .9896       .7177     37.96       .3545      .5230     1.0091     31.27      .1579      31.27
    .1654      .9911       .7043     37.76       .3680      .5303     1.0025     30.20      .1654      30.20
    .1730      .9938       .6907     37.55       .3828      .5368     1.0042     29.18      .1730      29.18
    .1807      .9900       .6769     37.33       .3982      .5402     1.1004     28.22      .1807      28.22
    .1830      .9894       .6720     37.26       .4043      .5413     1.1016     27.94      .1830      27.84
*JOB DONE*
     END  BREAK
      .179 CP SECONDS EXECUTION TIME
..
```